CHAPTER 8

Large-Scale Processing and Field Demonstration of High Early Strength Cementitious Composites in Bridge Repair

This chapter shifts the focus from "repair system durability assessment" to the "structural application" portion of the integrated engineering methodology (upper triangle in Figure 1.10). Efforts are made to transfer innovative ECC repair technology from the laboratory to field implementation through a bridge patch repair demonstration project. Large-scale processing and construction of an HES-ECC repair using commercial facilities are realized through optimization of the HES-ECC ingredients and mixing procedure, trial batches, and quality control methods. A simple lifecycle cost analysis is also performed to show the relative economic advantage of HES-ECC compared with concrete and alternative field repairs. The long-term durability of the HES-ECC patch repair under field conditions is monitored. Through this work, the linkages between material engineering, repair system durability assessment, and structural application are further forged.

8.1 Background

Before the newly-developed HES-ECC material can be considered as a viable building material for use in repair or structural designs, it must be capable of onsite processing and placement with adequate fresh properties and controlled quality at a large scale, using commercial batching and handling equipments common within the repair construction industry.

Large-scale mixing of ECC has been investigated in Japan[1] for pre-casting and spraying applications, and Michigan[2,3] in a UM (University of Michigan) - MDOT (Michigan Department of Transportation) project "Field Demonstration of Durable Link Slabs for Jointless Bridge Decks Based on Strain-Hardening Cementitious Composites". These investigations, especially those done in Michigan, provided good insights into large-scale mixing processes for the newly developed HES-ECC material.

Kanda et al.[1] investigated the tensile properties of ECC material produced using a 1.3 cubic yard (1 cubic meter) omni-mixer. This mixer is a force-based type that uses external mixing paddles to deform a rubber drum containing the cementitious material. This mixing equipment is substantially different from gravity mixers that rely mainly on gravity to mix a viscous liquid (paddles within the rotating drum lift the material and agitate it by dropping the material inside the drum). Force based mixers are typically much more efficient in achieving homogeneity within concrete mixes because of the greater mixing agitation. However, they are only common at pre-cast concrete plants, but very uncommon on construction sites where repair work is carried out. Gravity mixers, instead, are more typical equipment on repair construction sites. The present work demonstrated and concluded that larger scale on-site production of ECC using a gravity

mixer was possible and the performance of the material was similar to that mixed in the lab. Additionally, other work by Kanda et al.[1] used both gravity and omni-mixers to process ECC material for spraying applications. This limited study concluded that the mechanical performance of ECC processed using an ordinary concrete gravity mixer was similar to that using an omni-mixer.

Large scale mixing of a typical version of ECC (M45) using concrete mixing trucks was carried out for the field demonstration of ECC link slabs for jointless bridge decks in Michigan[2]. Before the truck mixing, grain size distribution analysis was conducted for proportioning the ECC components to produce a free-flowing mixture. The length of PVA fiber was changed from 0.5 in. (12.7 mm), as used previously in ECC M45, to 0.33 in. (8.4 mm) to promote easier mixing and better fiber dispersion in a gravity mixer. A local concrete supplier was then contracted to process 1, 2 and 4 cubic yard (0.76, 1.53, and 3.10 cubic meter) trial batches of ECC M45 material, which provided meaningful lessons for the following processing of 20 cubic yards (15.3 cubic meters) of ECC M45 for the construction of ECC link slabs. In total, based on mixings ranging from 1 cubic foot up to 20 cubic yards (0.03 to 15.3 cubic meters), it was concluded that large-scale mixing of ECC was able to produce fresh material that was homogeneous, rheologically stable, and had good flowability. Testing of mechanical properties of the hardened ECC M45 from the large-scale batches showed that the material compressive properties were similar to those of laboratory mixes, while the material tensile properties were reduced by an acceptably small amount from those typically seen in laboratory-grade ECC M45 material[2,3].

The material mix proportions of the ECC mix from Kanda et al.[1], ECC M45, and HES-ECC are compared in Table 8.1.

Compared with the other two ECC mixes that were previously investigated, HES-ECC contained a much higher content of cement, and no fly ash. In addition, the cement type was high early strength Portland type III cement rather than normal strength Portland type I cement, and the former had finer-sized particles (Blaine Surface area 2637 ft^2/lb (540 m^2/kg) for type III versus 1806 ft^2/lb (370 m^2/kg) for type I), resulting in a different fresh rheology and shorter setting time after mixing with water. Furthermore, an accelerator was used in HES-ECC that further shortened setting time, which put a tight constraint on the working time. Finally, HES-ECC included polystyrene beads, which affect the material fresh rheology (i.e. flowability, plastic viscosity, setting time) and dispersion of fibers. These four distinguishing features of HES-ECC compared with regular ECC pose extra challenges for its larger scale processing.

8.2 Optimization of HES-ECC Ingredients and Mixing Procedure for Larger Scale Applications

8.2.1 Fiber Length Change

Prior to conducting larger scale HES-ECC batching, the fresh rheology of HES-ECC was optimized to adapt to large gravity mixers. To achieve better flowability and more homogeneous fiber distribution, a change of fiber length was examined. The standard poly-vinyl-alcohol (PVA) fiber used in HES-ECC was 0.5 in. (12 mm) long and 1.5 mils (0.039 mm) in diameter. After adding the fibers to the fresh HES-ECC mortar, a significant increase in viscosity and reduction in flowability of the material was observed.

To improve the flowability of fresh HES-ECC, shorter PVA fibers with length of 0.33 in. (8 mm) and diameter of 1.5 mils (0.039 mm) were used to replace the 0.5 in. (12 mm)-long fibers. The two types of fibers (Figure 8.1) were identical with respect to chemical composition, surface coating, strength, and modulus.

The fresh-state flowability and the hardened mechanical properties of HES-ECC material using shorter fibers were measured. A flowability test[4] was performed on the fresh HES-ECC mix immediately after processing the material using a laboratory force-based mixer with 12 L capacity. In this test, a standard concrete slump cone was filled with fresh HES-ECC material and emptied onto a level sheet of Plexiglas. The flowable HES-ECC mix then flattened, only by gravity, into a large pancake-shaped mass. Two orthogonal diameter measurements of this "pancake" were recorded and averaged, denoted as D_1, which captured the overall deformability, or flowability, of the material in its fresh state. The flowability test showed that D_1 of HES-ECC increased from 22 in. to 24 in. (559 mm to 610 mm) by changing from 0.5 in. (12 mm)-long fibers to 0.33 in. (8 mm)-long fibers. This additional flowability of HES-ECC material allowed for easier mixing in large capacity gravity mixers and easier placement on the construction site.

Based on separate analytical studies[5], this fiber length change was shown to have a minimal effect on the crack bridging stress versus crack width opening curve $\sigma(\delta)$ and, therefore, little expected effect on the overall pseudo-tensile strain-hardening behavior of the ECC composite. To verify this, the tensile properties of HES-ECC with shorter fibers were evaluated using a uniaxial tensile test, as described in earlier chapters. HES-ECC specimens containing shorter fibers were demolded at 4h, cured in air, and tested at different ages from 4h to 28d. Three specimens were tested at each age. Table 8.2 summarizes the measured tensile properties at different ages, and Figure 8.2 shows the

typical stress-strain curves at different ages. It was observed that when shorter fibers were used, HES-ECC maintained tensile strain capacity of more than 3% at all ages. Therefore, the 0.33 in. (8 mm) fibers were selected for use in the larger scale batching.

8.2.2 Hydration Stabilizing Admixtures

As a gravity mixer instead of a force-based mixer is generally used on repair construction sites, longer mixing and working times should be necessary in achieving homogeneity and handling of HES-ECC. Due to a very high amount of type III cement and incorporation of hydration accelerator, HES-ECC set quickly after mixing was finished. Additionally, HES-ECC included Glenium 3200 HES admixture as the high-range water-reducing admixture, which was originally developed for extremely high early strength concrete. The slump retention of HES-ECC containing Glenium 3200 HES admixture was less than that of ECC M45 containing a conventional high-range water-reducing admixture. For all of the above reasons, HES-ECC began to lose its flowability and workability beyond the first 15-20 minutes after mixing was complete. Although such a short setting time would pose no major problems for small-scale specimens prepared for laboratory testing, this rapid loss of workability is not adequate for larger scale construction repairs. Therefore, a hydration-retarding admixture was needed to delay hydration at the very beginning and to extend setting when a longer working time was desirable, without sacrificing the early-age compressive strength gain rate.

A number of hydration retarders are commercially available. For this project Delvo® Stabilizer from MasterBuilders was selected due to its compatibility with the

accelerator Pozzolith® NC 534 and the superplasticizer HRWR Glenium® 3200HES used in HES-ECC. All three admixtures were produced by the same company. As declared by MasterBuilders, Delvo® Stabilizer can reduce water content as required to allow workability and reduce segregation. Additionally, it has been found that concrete produced with Delvo® Stabilizer can develop higher early-age (within 24 hours) and late-age compressive strengths than plain concrete when used within the recommended dosage range, and under normal curing conditions.

In the present study, dosage of Delvo® Stabilizer in HES-ECC followed the manufacturer's recommendation as 5 fl oz/cwt (65.2 mL/100 kg = 1.0 oz/cwt; cwt = hundredweight, or 100 pounds) of cementitious materials. HES-ECC containing stabilizer as well as shorter fibers was mixed using a laboratory force-based mixer, and the change in flowability with time was measured. As shown in Figure 8.3, HES-ECC without stabilizer exhibited rapid loss of flowability and became hardly workable after 15-20 minutes. However, HES-ECC with stabilizer exhibited a higher flowability and prolonged setting time, which was desirable for onsite larger-scale processing and handling. Table 8.3 summarizes the mixing proportions and batching weights of HES-ECC containing shorter fibers and hydration stabilizer.

8.2.3 Batching Sequence

To scale up HES-ECC batching from small laboratory mixers to large gravity mixers, the mixing sequence must be optimized to promote the best homogeneity of the material. In typical laboratory mixing, for which a force-based mixer was used, all dry ingredients of the HES-ECC matrix (cement and sand) were initially added to the mixer

and blended. Following a complete mixing of dry ingredients, water and high range water reducer were slowly added to gradually turn the mixture into a liquid state. Fibers were then slowly added and dispersed throughout the mixture. The accelerator was then added. Finally polystyrene beads were slowly added and mixed until they were well distributed. The overall mixing sequence lasted between 10 and 15 minutes.

For larger-scale mixing, however, the processing sequence described above was not applicable. Adding all of the dry components, including cement, followed by a small amount of water (due to the low water/cement ratio) resulted in a large mass of very dry material, which was difficult for a low-energy gravity mixer to process. Subsequently adding high range water reducer did not help to convert the dry mix into a liquid state, mainly due to the low speed and energy of the gravity mixer. Therefore, it was found to be essential that the mixture remained in a liquid state as long as possible throughout the mixing process and attained its most viscous state at the end of mixing. To meet this objective, the processing sequence using gravity mixers (with 2 cubic feet and 9 cubic feet capacities) was adjusted so that first all of the dry sand was added, along with three quarters of the water and all of the superplasticizer, as well as the stabilizer. Once these four components were well mixed, cement was added and mixed until the complete mortar matrix of ECC achieved a homogenous liquid state. The remaining mix water was then added with half of the accelerator admixture to wash the cement particles off the wall of the mixing drum. Fibers were subsequently added gradually into the mixture and mixed until they were well dispersed. Polystyrene beads were then added slowly and mixed until they were well distributed. In the end, the remaining half of the accelerator admixture was added until the complete material was homogenous and ready for

placement. This mixing sequence, which took 25 minutes in total, is shown with summaries of the time elapsed for each mixing step in Table 8.4.

8.3 HES-ECC Larger Scale Trial Batching

8.3.1 One Cubic Feet Batching

The goal of this one cubic foot (0.03 cubic meter) batching was to verify the applicability of the new mixing sequence of HES-ECC in a small gravity mixer with capacity of 2 cubic feet (0.06 cubic meters), as shown in Figure 8.4, and to examine the material's fresh and hardened properties when including 0.33 in. (8.4 mm) fibers and hydration stabilizer. Figure 8.5 illustrates the major mixing steps. The whole mixing process went as anticipated, validating the applicability of the suggested batching sequence for 1 cubic feet (0.03 cubic meters) batching of HES-ECC.

A flowability test was conducted on the fresh HES-ECC from the one cubic foot (0.03 cubic meter) batching, and the results are shown in Table 8.5 and Figure 8.6. The rate of reduction in flowability with time was similar to that of HES-ECC processed using the laboratory force-based mixer, as shown in Figure 8.3.

HES-ECC compressive cylinder specimens and tensile coupon specimens were cast from the one cubic foot (0.03 cubic meter) batch and tested for hardened mechanical properties at different ages. Compressive testing was done according to the ASTM C39 "Standard Test Method for Compressive Strength of Cylindrical Concrete Specimens" on standard 4 in. × 8 in. (102 mm × 203 mm) cylinders. Three specimens were tested for each test series. From the compressive test results summarized in Table 8.6 and Figure

8.7, it can be seen that HES-ECC processed from one cubic foot (0.03 cubic meter) batching was able to achieve the target compressive strength at both early and late ages.

Uniaxial tensile tests were conducted on HES-ECC tensile plate specimens cast from the one cubic foot (0.03 cubic meter) batch, with the same specimen size and test setup described in previous chapters. Three specimens were tested for each test series and their tensile properties are summarized in Table 8.7. Figure 8.8 shows representative tensile stress-strain curves of the HES-ECC mix at different ages. It can be seen that HES-ECC processed from one cubic foot (0.03 cubic meter) batching was able to achieve the target >2% tensile strain capacity at both early and late ages.

8.3.2 Three Cubic Feet Batching and Six Cubic Feet Batching

3 and 6 cubic feet (0.08 and 0.17 cubic meter) batches of HES-ECC were produced using a larger gravity mixer with capacity of 9 cubic feet (0.25 cubic meters), as shown in Figure 8.9. The processing steps are illustrated in Figure 8.10. As expected, due to the absence of large aggregates to agitate materials within the mixing drum, additional mixing time was needed between charging of the cementitious materials and the fibers. This added 5 to 10 minutes of mixing time provided further agitation and time for the high-range water-reducer to liquefy the material. Upon completion of mixing, the HES-ECC material for both batch sizes was evaluated for fiber distribution, flowability and mixture rheology. Fiber dispersion was evaluated through visual inspection and random sampling of the material to look for pockets or conglomerates of unmixed matrix materials or fiber bundles. Both batches produced close to homogenous material without segregation.

For the 3 cubic feet (0.08 cubic meter) batching, after achieving a homogenous HES-ECC mix, a small additional amount of superplasticizer was added to evaluate the possibility of further increasing the material's flowability. However, segregation was observed after adding the extra superplasticizer. Therefore, the mixed HES-ECC material was disposed of and was not evaluated for its compressive and tensile properties. From this experience, it was concluded that flowability higher than D_1=30 in. (762 mm) of HES-ECC without segregation could not feasibly be achieved, if no additional admixtures (e.g. viscosity modifying agents) are included. Therefore, the following 6 cubic feet (0.17 cubic meter) batching strictly followed the mixing proportions specified in Table 8.3.

Evaluation of the fresh HES-ECC from the 6 cubic feet (0.17 cubic meter) batching was done through flowability testing of the material. For this test, a standard concrete slump cone was filled with fresh HES-ECC and the cone was then removed, resulting in a "pancake" as shown in Figure 8.10 (f). The average deformation diameter D_1 was 24 in. (610 mm). The flowability test results are summarized in Table 8.5. The loss of deformability of HES-ECC processed in six cubic feet (0.17 cubic meter) batching is shown in Figure 8.11.

Similar to the 1 cubic feet (0.03 cubic meter) batching, HES-ECC compressive cylinder specimens and tensile coupon specimens were cast from the 6 cubic feet (0.17 cubic meter) batch and tested for hardened mechanical properties at different ages. Three specimens were tested for each test series. The compressive test results are summarized in Table 8.6 and Figure 8.12. The tensile test results are summarized in Table 8.7 and Figure 8.13. It was concluded that HES-ECC processed from the 6 cubic feet (0.17 cubic

meter) batching was able to achieve the target compressive strength and tensile strain capacity at both early and late ages.

The scaled up batching of HES-ECC demonstrated the success of the modified HES-ECC mix design and processing procedure. The specifications on quality control for constructing an HES-ECC repair are listed in Li et al. 2006[6].

8.4 HES-ECC Material Cost Effectiveness

The material costs (not including installation cost) of HES-ECC compared with various traditional or new repair materials are compared as below:

Portland cement concrete: \$80/yard^3 (\$105/m^3)

Steel fiber reinforced concrete: \$195/yard^3 (\$255/m^3)

High strength concrete: \$200/yard^3 (\$262/m^3)

Latex modified concrete: \$275-\$300/yard^3 (\$360-\$392/m^3)

Gypsum based patching material: \$415/yard^3 (\$543/m^3)

Normal PVA-ECC: \$220/yard^3 (\$288/m^3)

Thoroc 10-60: \$595 /yard^3 (\$778/m^3)

HES-ECC: \$615/yard^3 (\$804/m^3)

Polymer concrete/mortar: \$2700/yard^3 (\$3531/m^3)

Ductal: \$3000/yard^3 (\$3924/m^3)

The relative high cost of HES-ECC mainly comes from the large amount of fine silica sand, PVA fibers, and accelerators used in the mixture. However, the HES-ECC repair is still expected to be cost effective compared with other repair materials, from the viewpoint of service life cost, and in some cases even first cost. First cost includes both

material cost and installation cost. It may also include crack sealing cost for concrete deck repairs, which appears to be an accepted practice. The HES-ECC material cost is \$615/yard^3 (\$804/m^3) currently, which is higher than Portland cement concrete (\$80/yard^3 (\$105/m^3)), high strength concrete (\$200/yard^3 (\$262/m^3)), Steel Fiber Reinforced Concrete (SFRC) (\$195/yard^3 (\$255/m^3), and Gypsum based patching material (\$415/yard^3 (\$543/m^3)). However, HES-ECC is similar to Thoroc 10-60, which is a very rapid-setting one-component cement mortar, and is much cheaper than many of the other currently used "high performance" repair materials, such as Ductal (\$3000/yard^3 (\$3924/m^3), marketed by LaFarge), and Polymer Concrete/Mortar (\$2700/yard^3 (\$3531/m^3)). It should be noted that repair material cost only occupies a small portion of the repair first cost. Research work done by the Virginia Department of Transportation[7,8] concluded that the major cost of current repair overlay construction derives from costs associated with labor, equipment, mobilization, and traffic control, and material cost is generally less than 10% of the total repair overlay cost. In addition, the construction of the composite steel/ECC deck of a cable-stayed bridge in Hokkaido, Japan cites the reduction of installed cost (construction speed and lower labor cost) as one reason behind the choice of ECC over other cementitious materials. Other reasons cited included durability (estimated 100 year service life) and low weight (40% reduction compared with normal concrete with thicker section). Therefore, despite that the material cost of HES-ECC is higher than that of concrete, high strength concrete and SFRC, the savings in labor and equipment costs related to decreased traffic control and congestion during shortened construction and curing time can minimize the first cost of HES-ECC repairs.

From the service life cost point of view, HES-ECC repairs are expected to last for

a significantly longer time, compared with repairs made from traditional mortar or concrete-type materials, which are brittle. As has been documented in previous chapters, an HES-ECC repair can effectively suppress repair surface cracking and repair/concrete interface delamination, reflective cracking, and chloride penetration, thereby preventing common deterioration in concrete repairs. The HES-ECC repair has also been demonstrated to have a significantly longer fatigue life. As a result, the large savings from reduced future maintenance and repairs should make HES-ECC very competitive economically.

A preliminary life cycle cost (LCC) analysis was conducted based on the following assumptions:

a) Deck patch repair incurs the following costs: material, chipping (removal of old material), traffic control and mobilization.

b) Other related tasks (e.g. pier repair) incur the following costs: material, chipping, forming, and mobilization.

c) Repair depth = 4 in. (102 mm); each cubic yard (0.03 cubic meters) of material converts to 9 square yards (7.53 square meters) of patch area.

d) Discount factor I=3%.

e) All numbers below are based on the following MDOT document:

http://www.michigan.gov/documents/MDOT_14aCSM_Workbook05_126884_7.xls

Materials:

Concrete patch material cost = \$115/yard^3 (\$150/m^3) [concrete material] + \$685/yard^3 (\$896/m^3) [repair premium charge] = \$800/yard^3 (\$1046/m^3)

HES-ECC patch material cost = \$615/yard^3 (\$804/m^3) [HES-ECC material] + \$685/yard^3 (\$896/m^3) [repair premium charge] = \$1300/yard^3 (\$1700/m^3)

Chipping:

Deck: \$125/yard^2 = \$1125/yard^3 (for 4 in. repair depth)

(\$149/m^2 = \$1471/m^3 (for 102 mm repair depth))

Pier: \$65/feet^2 = \$1755/yard^3 (for 4 in. repair depth)

(\$700/m^2 = \$2295/m^3 (for 102 mm repair depth))

Forming:

\$28/feet^2 = \$2268/yard^3 (for 4 in. repair depth)

(\$301/m^2 = \$2966/meter^3 (for 102 mm repair depth))

Traffic control:

Assuming traffic control related cost is \$3000/day; patch repairs typically require 2 days, therefore traffic control related cost = \$6000.

Mobilization:

5% of all other costs.

Based on assumptions a) – e), the following calculation can be performed:

Deck patch repair cost per cubic yard:

Normal concrete patch repair: \$800/yard^3 (\$1046/m^3) [material] + \$1125/yard^3 (\$1471/m^3) [chipping] + \$6000/yard^3 (\$7848/m^3) [traffic] + \$396/yard^3 (\$518/m^3) [mobilization] = \$8320/yard^3 (\$10882/m^3)

HES-ECC patch repair: \$1300/yard^3 (\$1700/m^3) [material] + \$1125/yard^3 (\$1471/m^3) [chipping] + \$6000/yard^3 (\$7848/m^3) [traffic] + \$421/yard^3 (\$551/m^3) [mobilization] = \$8846/yard^3 (\$11570/m^3)

Other than deck patch repair cost per cubic yard:

Normal concrete patch repair: \$800/yard^3 (\$1046/m^3) [material] + \$1755/yard^3 (\$2295/m^3) [chipping] + \$2268/yard^3 (\$2966/m^3) [forming] + \$241/yard^3 (\$315/m^3) [mobilization] = \$5064/yard^3 (\$6600/m^3)

HES-ECC patch repair: \$1300/yard^3 (\$1700/m^3) [material] + \$1755/yard^3 (\$2295/m^3) [chipping] + \$2268/yard^3 (\$2966/m^3) [forming] + \$266/yard^3 (\$348/m^3) [mobilization] = \$5589/yard^3 (\$7310/m^3)

The question to be discussed here is: Assuming the service life of a normal concrete patch is 3 or 10 years, how long must an HES-ECC patch last for its life cycle cost to equal that of a normal concrete patch?

Deck patch repair

(a) Assumption Case 1: Normal concrete patch life = 3 years

Assuming the present value of LCC of a normal concrete deck patch with service life of 3 years equals to the present value of LCC of a HES-ECC deck patch with service life of x years:

$$\$8320 + \frac{\$8320}{(1+3\%)^3} + \frac{\$8320}{(1+3\%)^6} + \frac{\$8320}{(1+3\%)^9} + \frac{\$8320}{(1+3\%)^{12}} + \frac{\$8320}{(1+3\%)^{15}} + ...$$
$$= \$8846 + \frac{\$8846}{(1+3\%)^x} + \frac{\$8846}{(1+3\%)^{2x}} + \frac{\$8846}{(1+3\%)^{3x}} + \frac{\$8846}{(1+3\%)^{4x}} + \frac{\$8846}{(1+3\%)^{5x}} + ...$$

By solving this equation we get x = 3.2 years

Therefore, the HES-ECC deck patch must last at least 3.2 years for its LCC to equal or be less than that of a normal concrete deck patch with service life of 3 years.

(b) Assumption Case 2: Normal concrete patch life = 10 years

Assuming the present value of LCC of a normal concrete deck patch with service life of 10 years equals the present value of LCC of a HES-ECC deck patch with service life of y years:

$$\$8320 + \frac{\$8320}{(1+3\%)^{10}} + \frac{\$8320}{(1+3\%)^{20}} + \frac{\$8320}{(1+3\%)^{30}} + \frac{\$8320}{(1+3\%)^{40}} + \frac{\$8320}{(1+3\%)^{50}} + ...$$
$$= \$8846 + \frac{\$8846}{(1+3\%)^{y}} + \frac{\$8846}{(1+3\%)^{2y}} + \frac{\$8846}{(1+3\%)^{3y}} + \frac{\$8846}{(1+3\%)^{4y}} + \frac{\$8846}{(1+3\%)^{5y}} + ...$$

By solving this equation we get y = 10.5 years

Therefore, the HES-ECC deck patch must last at least 10.5 years for its LCC to equal or be less than that of a normal concrete deck patch with service life of 10 years.

Non-deck patch repair

(a) Assumption Case 1: Normal concrete patch life = 3 years

Assuming the present value of LCC of a normal concrete non-deck patch with service life of 3 years equals the present value of LCC of a HES-ECC non-deck patch with service life of x years:

$$\$5064 + \frac{\$5064}{(1+3\%)^{3}} + \frac{\$5064}{(1+3\%)^{6}} + \frac{\$5064}{(1+3\%)^{9}} + \frac{\$5064}{(1+3\%)^{12}} + \frac{\$5064}{(1+3\%)^{15}} + ...$$
$$= \$5589 + \frac{\$5589}{(1+3\%)^{x}} + \frac{\$5589}{(1+3\%)^{2x}} + \frac{\$5589}{(1+3\%)^{3x}} + \frac{\$5589}{(1+3\%)^{4x}} + \frac{\$5589}{(1+3\%)^{5x}} + ...$$

By solving this equation we get y = 3.3 years

Therefore, the HES-ECC non-deck patch must last at least 3.3 years for its LCC to equal or be less than that of a normal concrete non-deck patch with life of 3 years.

(b) Assumption Case 2: Normal concrete patch life = 10 years

Assuming the present value of LCC of a normal concrete non-deck patch with life of 10 years equals to the present value of LCC of a HES-ECC non-deck patch with life of y years:

$$\$5064 + \frac{\$5064}{(1+3\%)^{10}} + \frac{\$5064}{(1+3\%)^{20}} + \frac{\$5064}{(1+3\%)^{30}} + \frac{\$5064}{(1+3\%)^{40}} + \frac{\$5064}{(1+3\%)^{50}} + ...$$
$$= \$5589 + \frac{\$5589}{(1+3\%)^{y}} + \frac{\$5589}{(1+3\%)^{2y}} + \frac{\$5589}{(1+3\%)^{3y}} + \frac{\$5589}{(1+3\%)^{4y}} + \frac{\$5589}{(1+3\%)^{5y}} + ...$$

By solving this equation we get y = 10.9 years

Therefore, the HES-ECC non-deck patch must last at least 10.5 years for its LCC to equal or be less than that of a normal concrete non-deck patch with life of 10 years.

The Thoroc 10-60 Rapid Mortar is a patch repair material used by MDOT. It is a very rapid-setting cement mortar containing crystalline silica, Portland cement, hydraulic cement and lithium carbonate. During the HES-ECC patch repair demonstration project, patch repairs made of Thoroc 10-60 and HES-ECC were poured side by side to compare their early-age and long-term performance. The material cost of Thoroc 10-60 is \$595/yard^3 (\$778/m^3), which is similar to the \$615/yard^3 (\$804/m^3) material cost for HES-ECC. Assuming the installation costs for HES-ECC and Thoroc 10-60 are the same, the preliminary LCC analysis shows that both the Thoroc 10-60 patch and the HES-ECC patch must last at least 3.2 years (deck patch) or 3.3 years (non-deck patch) for their LCC to equal or be less than that of a normal concrete patch with service life of 3 years; both the Thoroc 10-60 patch and the HES-ECC patch must last at least 10.5 years (deck patch) or 10.9 (non-deck patch) for their LCC to equal or be less than that of a normal concrete patch with service life of 10 years.

The above LCC calculations suggested that regarding economic cost, the use of HES-ECC is preferable to other repair materials if the repair service life can be extended by approximately 10%. The findings from previous chapters of this dissertation suggested that service life of a HES-ECC patch repair should be significantly longer than traditional concrete repairs, thus justifying the cost effectiveness of HES-ECC as a patch repair material.

Note that the above analyses do not account for user or environmental costs. If these costs were accounted for, the longer service life of HES-ECC over other repair materials would give additional advantage to HES-ECC.

8.5 HES-ECC Patch Repair Demonstration

Construction of a patch repair on the Ellsworth Road Bridge over US-23 (S07 of 81074), Ann Arbor, Michigan began at 9am on Tuesday, November 28, 2006 with placement of traffic control devices. Photographs of the construction process are shown in Figures 8.15 – 8.28. The MDOT repair personnel conducted partial depth concrete removal, sandblasted the patch area, replaced damaged reinforcement, and completed patch preparation. Before pouring the patch materials, water fog was sprayed onto the concrete substrate to enhance repair bonding. The average temperature was 55 °F (12.8 °C) and relative humidity was 59.5% during this construction.

HES-ECC mixing materials were pre-packed in the laboratory for easy field processing, and then transported to the repair site. 7 cubic feet (0.20 cubic meter) HES-ECC was mixed by UM research personnel using a 12 cubic feet (0.34 cubic meter) capacity concrete gas mixer provided by MDOT (Figure 8.22). The total mixing time

was approximately 30 minutes. The fresh HES-ECC exhibited desirable viscosity, fiber distribution and flowability (Figure 8.25). Flowability testing using a slump cone was conducted immediately after finishing the mixing and before repair placement. With a 25.6 in. (650.2 mm) slump diameter, the HES-ECC achieved a self-compacting state. The HES-ECC material was then poured into a wheelbarrow, transported to the patch area, and poured into the patch. The self-compacting property of HES-ECC allowed it to easily flow into the corners of the patch area without any vibration. The surface of the HES-ECC patch repair was finalized by using a steel trowel, by hand.

Mixing of Thoroc 10-60 was performed by MDOT personnel using the same mixer as for mixing HES-ECC. It can be seen from Figure 8.26 that the fresh Thoroc 10-60 was barely flowable, resulting in much more effort and a longer time for construction workers to place and finish. The two patch repairs using HES-ECC and Thoroc 10-60 are shown side-by-side in Figure 8.27. Latex-based curing compound was sprayed onto both patches to reduce evaporation and shrinkage.

The two side-by-side patch repairs on the Ellsworth Road Bridge were completed at around 1pm on Tuesday, November 28, 2006, as shown in Figure 8.28. Traffic reopened at 9am on Wednesday, November 29, 2006.

8.6 Long-Term Monitoring of HES-ECC Patch Repair Performance

After placement, the HES-ECC and Thoroc 10-60 patch repairs were exposed to identical traffic and environmental loads, thereby allowing for a comparison of their long-term durability performance. (The HES-ECC patch was on the shoulder lane and therefore experienced less severe direct traffic loading.) The bridge has a high average

daily traffic (ADT) of 22,546, and it is also used frequently by 11-axle trucks that are heavily loaded with aggregates. Hence, mechanical (traffic) loading on the patch repairs is significant. Potential environmental loading (S.E. Michigan weather exposure) on the patch repairs includes shrinkage, temperature change, freezing and thawing, chloride penetration, salt scaling and potential steel corrosion.

The performance of the HES-ECC and adjacent Thoroc 10-60 patch repairs has been assessed through a series of twelve site visits. The initial visit was 1 day after construction (November 29, 2006). The last visit was on September 18, 2009. The maximum surface crack width and maximum interfacial delamination width of the HES-ECC and Thoroc 10-60 patch repairs at different ages are plotted in Figure 8.29 and 8.30. Several microcracks with width of 60 μm were observed in the HES-ECC patch 2 days after construction. After nearly 3 years of service (November 2006 - September 2009), the width of microcracks in the HES-ECC patch remain less than 90 μm, although more microcracks have been found over time. The interfacial delamination width between the HES-ECC patch and existing concrete is less than 70 μm. For the Thoroc 10-60 patch repair, several cracks with maximum crack width of 300 μm were observed 34 days after construction, and the maximum crack width increased to 1700 μm at the time of the last visit (September 2009). Microspalling was also observed at some crack locations. The interfacial delamination width between the Thoroc 10-60 patch and existing concrete was 900 μm 34 days after construction, and increased to 2200 μm at the time of the last visit. Therefore, at the same age of approximately 2 years and 10 months, and under the given mechanical and environmental loading conditions, the maximum surface crack width and maximum interfacial delamination width of the HES-ECC patch were both much smaller

than in the Thoroc 10-60 patch (Figure 8.31, 8.32, 8.33, 8.34, 8.35). Furthermore, exposure of aggregates in the Thoroc 10-60 patch repair was observed close to the Thoroc 10-60/HES-ECC interface area, while no disintegration in the HES-ECC patch was observed (Figure 8.35). No spalling or other deterioration has been found in the HES-ECC patch to date.

This field performance data for 2 years and 10 months of patch life reveals the promise of HES-ECC as a durable repair material in the harsh environments of Michigan winters (with combined effects of restrained shrinkage, freezing and thawing, exposure to de-icing salts, temperature change, etc.) in addition to heavy traffic loads. The performance of the HES-ECC patch repair and Thoroc 10-60 patch repair on Ellsworth Road Bridge, Michigan, will continue to be monitored and reported in future publications.

8.7 Conclusions

Within this work, the design and optimization of HES-ECC ingredients and a processing procedure for large-scale commercial batching were completed. These included the reduction of fiber length from 12 mm to 8 mm, incorporation of a hydration stabilizing admixture, and revision of the mixing sequence. The three scaled-up trial mixtures of 1, 3, and 6 cubic feet using gravity mixers verified that larger-scale onsite mixing of HES-ECC is feasible and can result in a material that is both high performance by retaining overall tensile ductility and microcracking behavior, and commercially producible using gravity mixer-based batching operations.

The capability of onsite large-scale processing and placement of HES-ECC was demonstrated in a bridge patch repair construction project on the Ellsworth Road Bridge

over US-23 (S07 of 81074) on November 28, 2006. The construction process went smoothly, and produced a close-to-homogeneous, self-compacting HES-ECC material that was easy to pour into the patch area without external vibration. Testing of mechanical properties of HES-ECC specimens made from the same batch showed that the compressive strength and tensile properties (tensile strain capacity, tensile strength, multiple microcracking behavior) were similar to those of laboratory mixtures. The repair construction was completed at around 1pm on Tuesday, November 28, 2006. Traffic reopened early at 9am on Wednesday, November 29, 2006.

A simple lifecycle cost analysis was also performed to show the relative economic advantage of HES-ECC compared with concrete and alternative field repairs. This analysis suggests that just a 10% increase in service life would lead to a lower life cycle cost if HES-ECC (with higher material cost) were adopted, compared with current patch repair materials.

The long-term durability of the HES-ECC patch repair under field conditions has been monitored up to approximately 2 years and 10 months after patch placement. Under heavy traffic loading, restrained shrinkage, temperature effects, three winters' exposure to freezing and thawing as well as de-icing salts, and other possible loading conditions in the field, the HES-ECC patch repair exhibited multiple microcracking behavior with crack width below 100 μm, repair/old interfacial delamination width no greater than 60 μm, and no sign of disintegration or fracture failure, which outperformed the adjacent Thoroc 10-60 patch repair constructed at the same time and which experienced the same loading conditions. While the shoulder lane placement favors the durability of the HES-ECC patch compared with the Thoroc 10-60 patch that was in the right hand driving lane,

the durable performance of HES-ECC shown in this patch repair was consistent with another patch repair made with ECC M45 (without the high early age strength) placed on Curtis Road in Ann Arbor, Michigan in 2002[9].

Overall, this work proved the capability of onsite large-scale processing and placement of HES-ECC using traditional equipment, and further validated the long-term durability of HES-ECC repairs under combined mechanical and environmental loading conditions under field conditions.

Table 8.1 – ECC material mixing proportions.

Material	**Kanda et al.**	**ECC – M45**	**HES-ECC**
Cement	1.0	1.0	1.0
Sand	0.91	0.8	1.0
Fly Ash	0.43	1.2	0.0
Water	0.65	0.53	0.33
PS Beads	0.0	0.0	0.064
High Range Water Reducer	0.0	0.03 Plastol 5000	0.0075 GL3200-HES
Accelerator	0.0	0.0	0.04
Anti-Shrinkage Agent	0.027	0.0	0.00
Fiber (Vol. %)	0.02	0.02	0.02

Table 8.2 – Tensile properties of HES-ECC with 0.33 in. (8.4 mm) PVA fiber.

Age	**Young's Modulus Ksi (GPa)**	**Ultimate Strength psi (MPa)**	**Strain Capacity (%)**
4h	1728.26 (11.9)	511.54 (3.53)	4.21
	1913.22 (13.2)	518.17 (3.57)	5.52
	1997.68 (13.8)	525.73 (3.62)	5.66
24h	2553.43 (17.6)	679.11 (4.68)	3.95
	2596.56 (17.9)	690.32 (4.76)	4.29
	2687.32 (18.5)	702.12 (4.84)	4.43
7d	2901.12 (20.0)	820.33 (5.66)	3.36
	2987.55 (20.6)	829.67 (5.72)	3.51
	3102.28 (21.4)	851.52 (5.87)	3.64
28d	3245.42 (22.4)	811.67 (5.60)	3.28
	3376.51 (23.3)	832.21 (5.74)	3.55
	3401.63 (23.5)	908.82 (6.27)	3.57

Table 8.3 – Larger scale HES-ECC mixing proportions and batching weights.

Material	**Proportion**	**Amount lb/yard^3 (kg/m^3)**
Cement	1.0	1547.37 (3.32×10^{-2})
Sand	1.0	1547.37 (3.32×10^{-2})
Water	0.33	507.54 (1.09×10^{-2})
PVA Fiber (Vol. %)	0.02	44.01 (9.45×10^{-4})
Polystyrene Beads	0.064	99.09 (2.13×10^{-3})
High Range Water Reducer	0.0075	11.61 (2.49×10^{-4})
Accelerator	0.04	61.83 (1.33×10^{-3})
Hydration Stablizer	0.0046	7.02 (1.51×10^{-4})

Table 8.4 – Larger scale HES-ECC batching sequence and time.

Activity	**Elapsed Time including Mixing Time (min)**
1. Charge all sand	2
2. Charge 3/4 amount of mixing water, all HRWR, and all hydration stabilizer	2
3. Charge all cement slowly	4
4. Charge remaining 1/4 amount of mixing water to wash drum	1
5. Charge 1/2 amount of accelerator, mix until the whole HES-ECC matrix material is homogenous	5
6. Charge PVA fibers slowly, mix until the fibers are well distributed	5
9. Charge PS beads slowly, mix until the beads are well distributed	4
10. Charge the remaining 1/2 amount of accelerator, mix until the complete material is homogenous and ready for placement	2
Total	25

Table 8.5 – Flowability test results from one & six cubic feet (0.03 & 0.17 cubic meter) batching using a gravity mixer.

Minute	Average Deformation Diameter, D_1 in. (mm)	
	One Cubic Foot	Six Cubic Feet
3	22.83 (580)	24.02 (610)
10	21.26 (540)	–
20	18.50 (470)	20.47 (520)
30	17.72 (450)	17.72 (450)
40	15.75 (400)	15.35 (390)

Table 8.6 – Compressive Strength development of HES-ECC from one & six cubic feet (0.03 & 0.17 cubic meter) batching using a gravity mixer.

Age	Compressive Strength psi (MPa)						
	Target	One Cubic Foot			Six Cubic Feet		
4 h	2500 (17.2)	2623 (18.1)	2718 (18.7)	2932 (20.2)	3012 (20.8)	2511 (17.3)	2732 (18.8)
6 h	3000 (20.7)	4876 (33.6)	5113 (35.3)	5428 (37.4)	5526 (38.1)	4722 (32.6)	5209 (35.9)
24 h	5000 (34.5)	6258 (43.1)	5873 (40.5)	6115 (42.2)	6211 (42.8)	5977 (41.2)	6289 (43.4)
28 d	7000 (48.3)	8621 (59.4)	8209 (56.6)	8012 (55.2)	8701 (60.0)	8454 (58.3)	8500 (58.6)

Table 8.7 – Tensile properties of HES-ECC from one & six cubic feet (0.03 & 0.17 cubic meter) batching using a gravity mixer.

Age		Young's Modulus ksi (MPa)	Ultimate Strength psi (MPa)	Strain Capacity (%)
One Cubic Foot	4h	1728 (11916)	512 (3.53)	4.21
		1913 (13191)	518 (3.57)	5.52
		1998 (13774)	526 (3.62)	5.66
	24h	2553 (17605)	679 (4.68)	3.95
		2597 (17903)	690 (4.76)	4.29
		2687 (18528)	702 (4.84)	4.43
	28d	3245 (22376)	812 (5.60)	3.28
		3377 (23280)	832 (5.74)	3.55
		3402 (23453)	909 (6.27)	3.57
Six Cubic Feet	4h	1812 (12493)	497 (3.43)	4.05
		1901 (13107)	522 (3.60)	4.53
		1979 (13645)	533 (3.67)	4.68
	6h	2000 (13790)	601 (4.14)	4.34
		2103 (14500)	619 (4.27)	4.52
		2210 (15237)	629 (4.34)	5.01
	24h	2499 (17230)	678 (4.67)	3.43
		2587 (17837)	689 (4.75)	3.55
		2713 (18705)	695 (4.79)	3.87
	28d	3302 (22766)	813 (5.61)	3.02
		3421 (23587)	826 (5.70)	3.26
		3499 (24125)	851 (5.87)	3.62

Table 8.8 – Minimum requirements of HES-ECC material.

Minimum Requirements of HES-ECC Material	4 hour	6 hour	24 day	28 day
Compressive Strength psi (MPa)	2500 (17.24)	3000 (20.68)	5000 (34.47)	7000 (48.26)
Tensile Strength [Uniaxial] psi (MPa)	400 (2.76)	500 (3.45)	600 (4.14)	700 (4.83)
Ultimate Tensile Strain Capacity [Uniaxial]	2%			

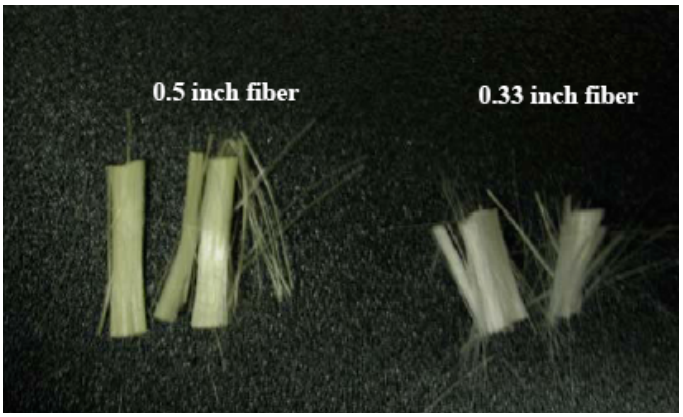

Figure 8.1 – PVA fiber, 0.5 in. (12.7 mm) and 0.33 in. (8.4 mm).

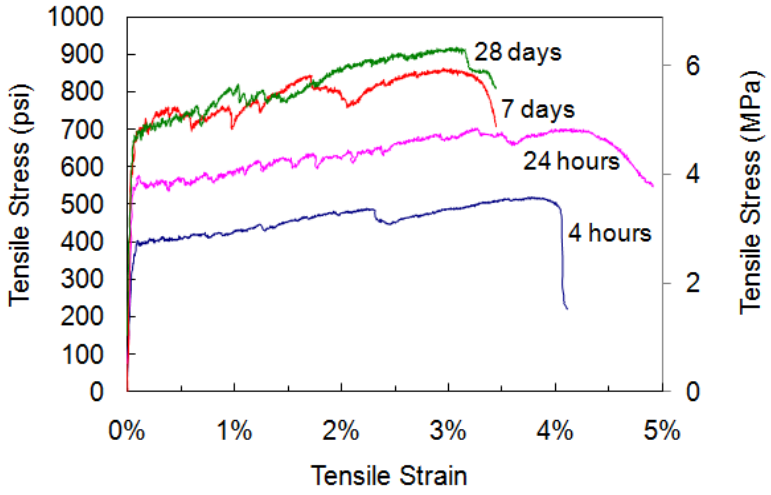

Figure 8.2 – Tensile stress-strain curves of HES-ECC with 0.33 in. (8.4 mm) PVA fiber.

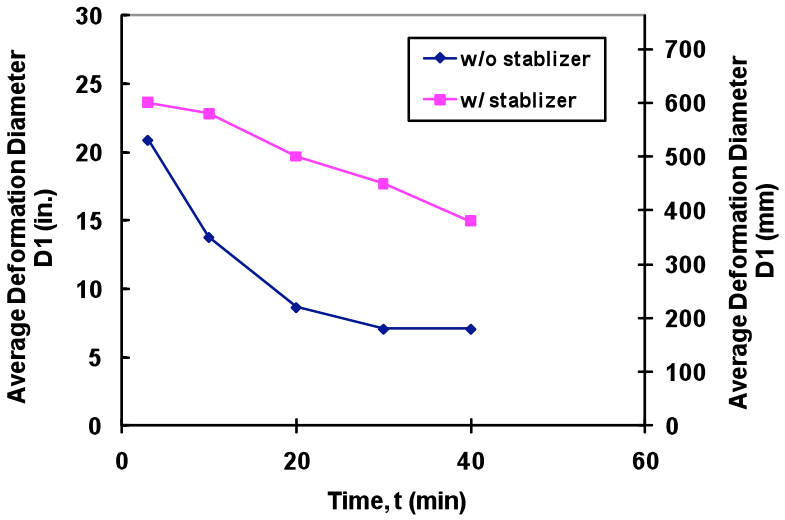

Figure 8.3 – Loss of deformability of HES-ECC with and without hydration stabilizer.

Figure 8.4 – Gravity mixer with capacity of two cubic feet (0.057 cubic meters).

a) After adding sand, water, HRWR and hydration stabilizer.

b) After adding cement (homogenous and creamy HES-ECC mortar matrix).

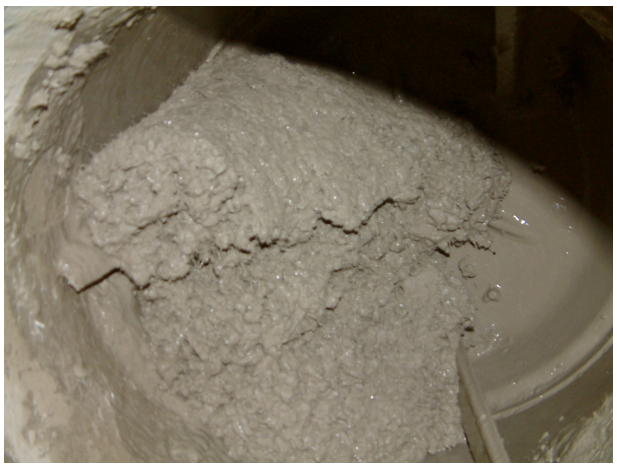

c) After adding PVA fibers.

d) After adding PS beads.

Figure 8.5 – HES-ECC one cubic feet (0.03 cubic meter) mixing.

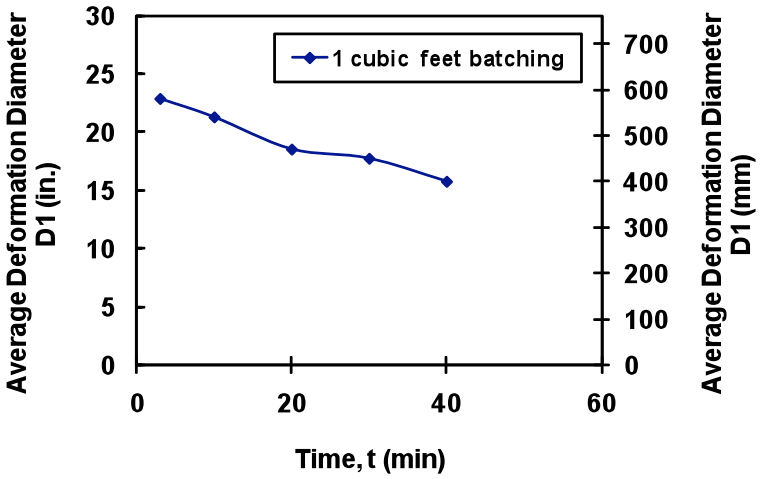

Figure 8.6 – Loss of deformability of HES-ECC processed in one cubic feet (0.03 cubic meter) batching.

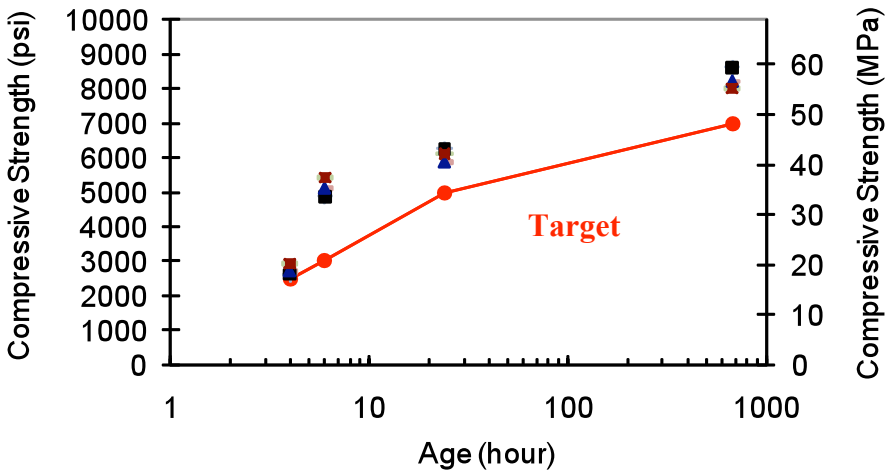

Figure 8.7 – Compressive strength development of HES-ECC from one cubic feet batching.

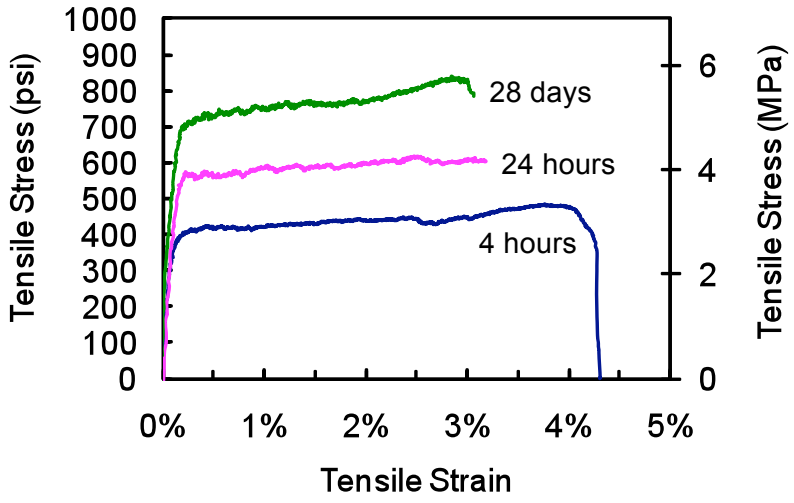

Figure 8.8 – Tensile stress-strain curves of HES-ECC from one cubic feet batching.

Figure 8.9 – Gravity mixer with capacity of 9 cubic feet (0.25 cubic meters).

a) Pre-wetting the mixer.

b) After adding sand, water, HRWR and hydration stabilizer.

c) After adding cement (homogenous and creamy HES-ECC mortar matrix).

d) After adding PVA fibers.

e) After adding PS beads.

f) Flowability test (5 minutes).

Figure 8.10 – HES-ECC six cubic feet (0.17 cubic meters) mixing.

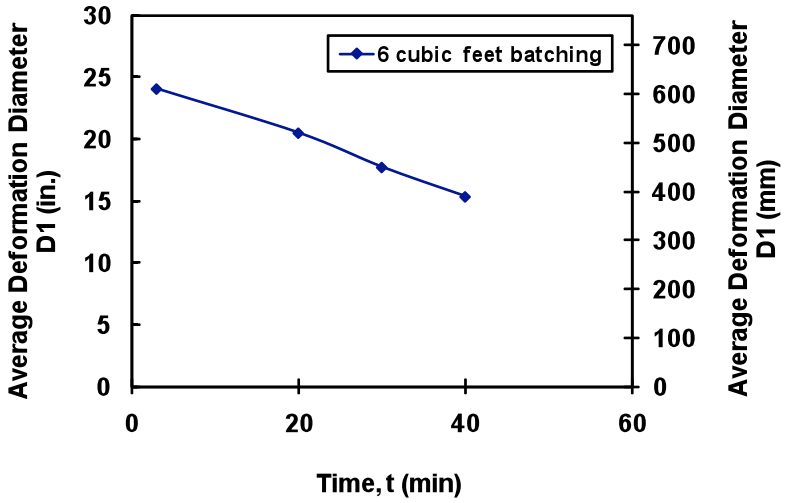

Figure 8.11 – Loss of deformability of HES-ECC processed in six cubic feet (0.17 cubic meters) batching.

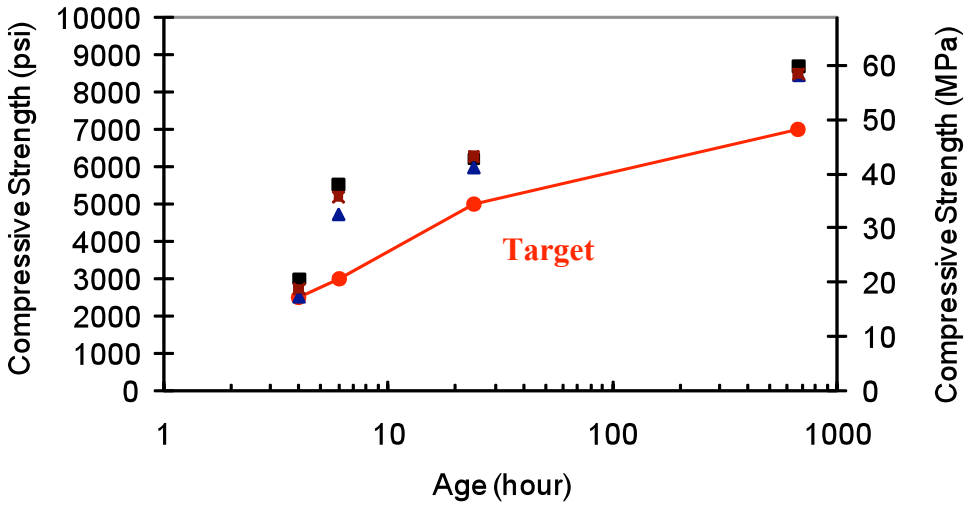

Figure 8.12 – Compressive strength development of HES-ECC from 6 cubic feet (0.17 cubic meter) batching.

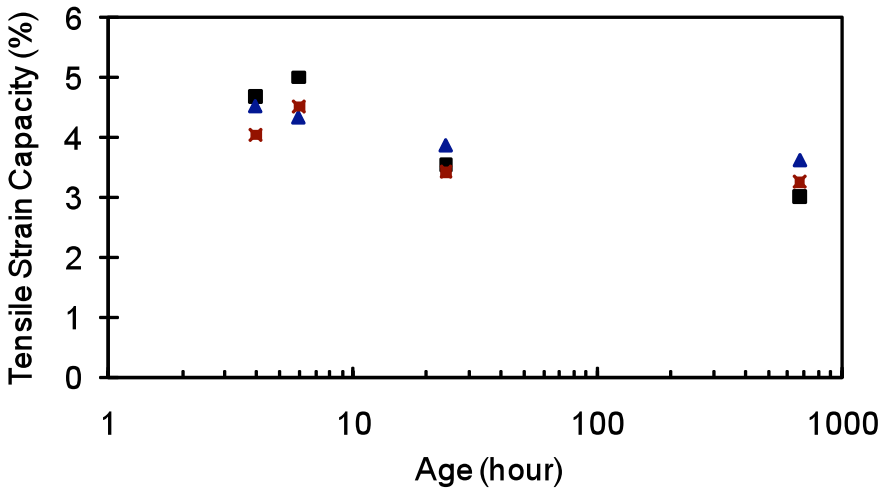

Figure 8.13 – Tensile strain capacity development of HES-ECC from 6 cubic feet (0.17 cubic meters) batching.

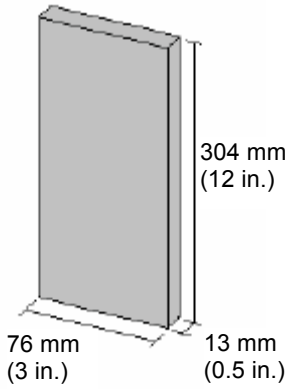

Figure 8.14 – Uniaxial tensile test plate dimensions.

Figure 8.15 – Ellsworth Road Bridge over US-23 (S07 of 81074).

Figure 8.16 – Bridge deck cracking.

Figure 8.17 – Partial depth removal.

Figure 8.18 – Sandblasting of patch area.

Figure 8.19 – Replacement of damaged reinforcement.

Figure 8.20 – Completed patch repair preparation.

Figure 8.21 – Separated patch areas for HES-ECC repair and Thoroc 10-60 repair.

Figure 8.22 – 12 cubic foot (0.34 cubic meter) capacity gas mixer.

Figure 8.23 – Pouring HES-ECC into wheelbarrow for transportation.

Figure 8.24 – HES-ECC was poured into patch.

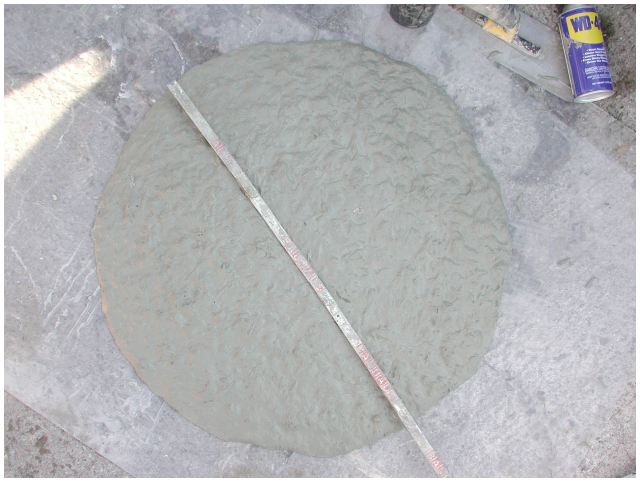

Figure 8.25 – HES-ECC shows self-compacting property.
(Flowability test slump diameter = 25.6 in. (650 mm))

Figure 8.26 – Placement of Thoroc 10-60.

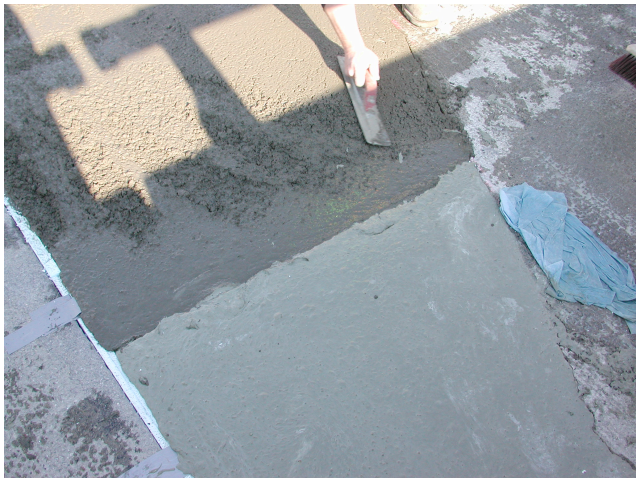

Figure 8.27 – Comparison of HES-ECC patch repair and Thoroc 10-60 patch repair.

Figure 8.28 – Completed patch repair work.

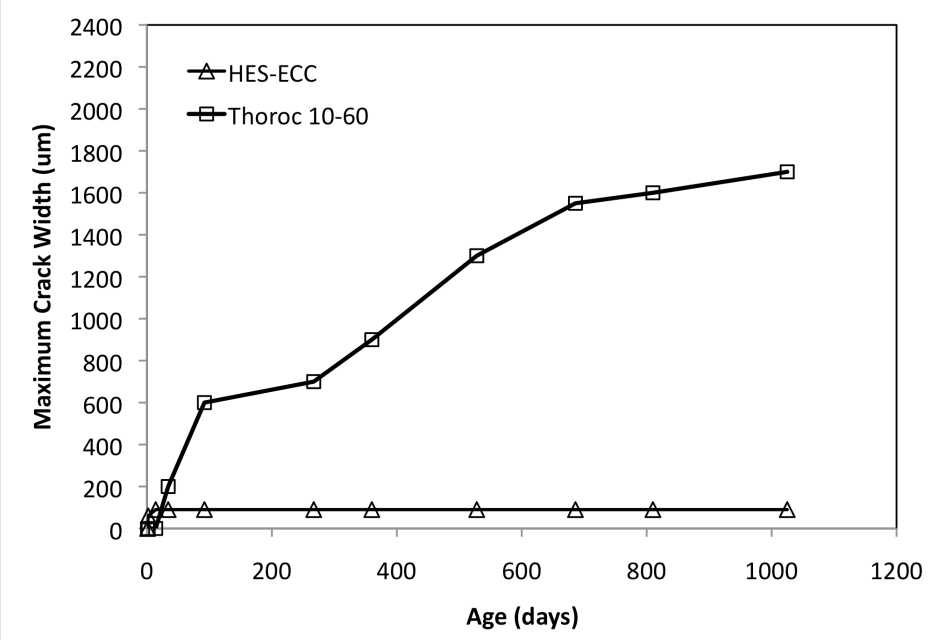

Figure 8.29 – Maximum surface crack width of HES-ECC and Thoroc 10-60 patch repairs.

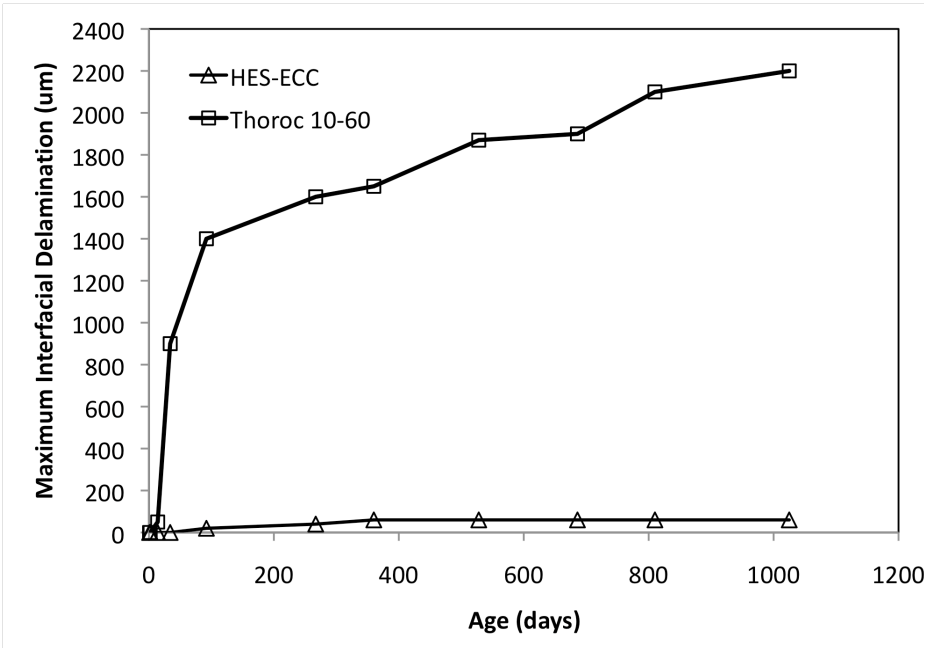

Figure 8.30 – Maximum interfacial delamination width of HES-ECC and Thoroc 10-60 patch repairs.

.

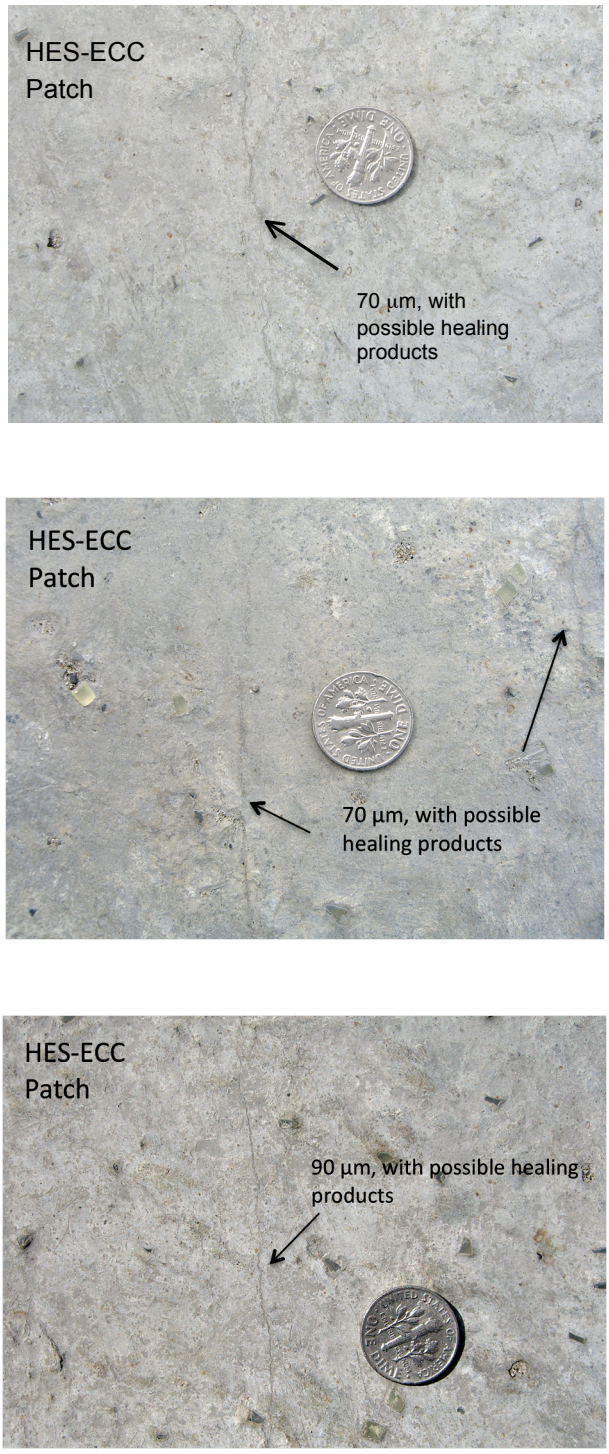

Figure 8.31 – Surface cracking in HES-ECC patch repair, on September 18, 2009.

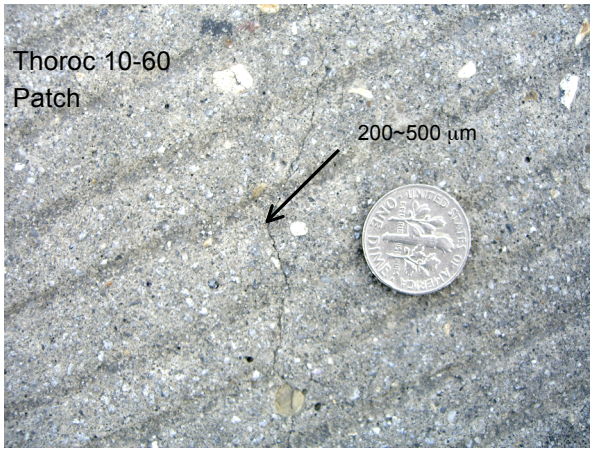

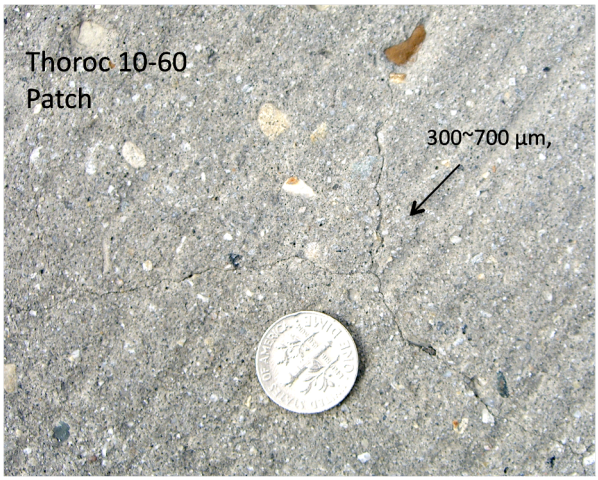

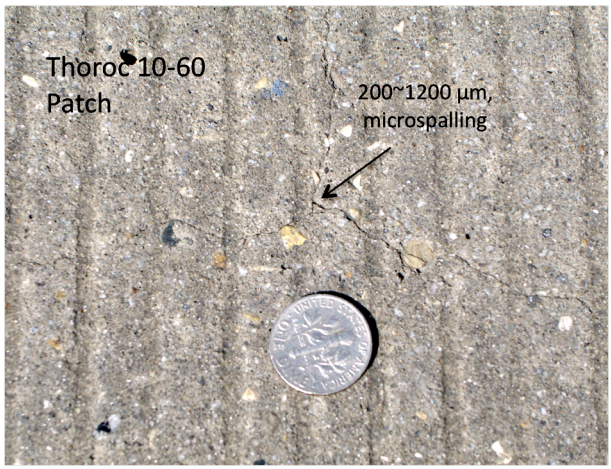

Figure 8.32 – Surface cracking in Thoroc 10-60 patch repair, on September 18, 2009.

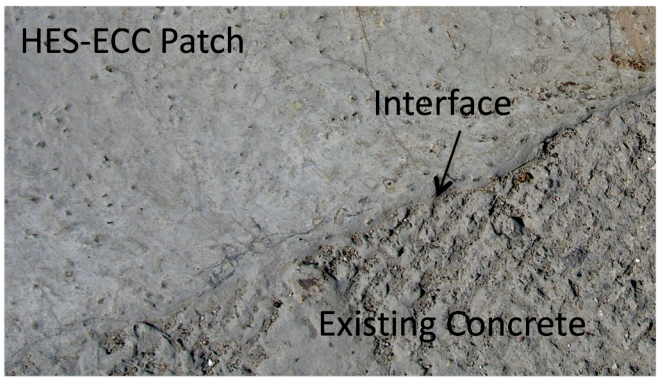

Figure 8.33 – Interfacial delamination between HES-ECC patch repair and existing concrete, on September 18, 2009.

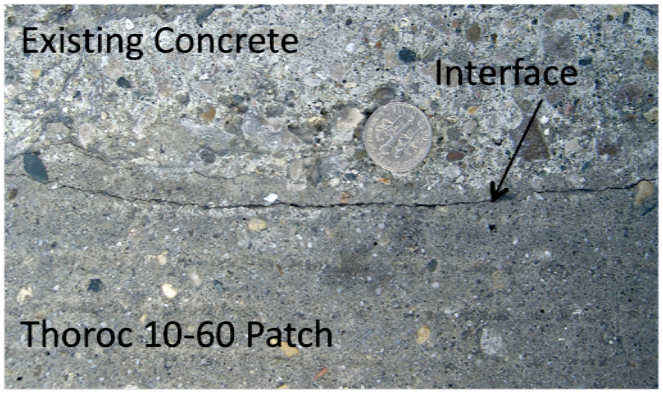

Figure 8.34 – Interfacial delamination between Thoroc 10-60 patch repair and existing concrete, on September 18, 2009.

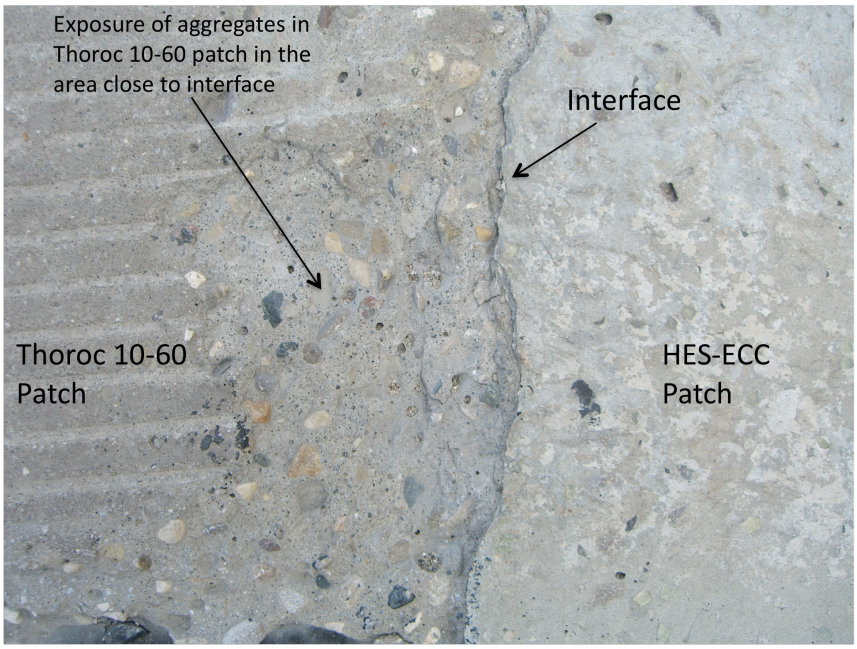

Figure 8.35 – Exposure of aggregates in Thoroc 10-60 patch repair close to the Thoroc 10-60/HES-ECC interface area, on September 18, 2009.

References:

[1] Kanda, T et al, "Tensile and Anti-Spalling Properties of Direct Sprayed ECC," *Journal of Advanced Concrete Technology*, Vol. 1, No. 3, 2003, pp. 269-282.

[2] Li, V. C., Lepech, M. and Li, M., "Final Report on Field Demonstration of Durable Link Slab for Jointless Bridge Decks Based on Strain-Hardening Cementitious Composites," Michigan Department of Transportation, 2005.

[3] Lepech, M.D., and Li, V. C., "Large Scale Processing of Engineered Cementitious Composites," *ACI Materials Journal*, Vol. 105, No. 4, 2008, pp. 358-366.

[4] Kong, J.H., Bike, S. and Li, V.C., "Development of a Self-Consolidating Engineered Cementitious Composite Employing Electrosteric Dispersion/Stabilization," *Journal of Cement and Concrete Composites*, Vol. 25, No. 3, 2003, pp. 301-309.

[5] Kanda, T. and V.C. Li, "Effect of Apparent Fiber Strength and Fiber-Matrix Interface on Crack Bridging in Cement Composites," *ASCE J. of Engineering Mechanics*, Vol. 125, No. 3, 1999, pp. 290-299.

[6] Li, V. C., Li, M. and Lepech, M., "High Performance Material for Rapid Durable Repair of Bridges and Structure," Michigan Department of Transportation, December 2006.

[7] Sprinkel, M., "Evaluation of Latex-Modified and Silica Concrete Overlays Placed on Six Bridges in Virginia," *Virginia DOT Final Report*, 2000. (a)

[8] Sprinkel, M., "Evaluation of High Performance Concrete Overlays Placed on Route 60 Over Lynnhaven Inlet in Virginia," *Virginia DOT Final Report*, 2000. (b)

[9] Li, V.C. and M. Li, "Durability Performance of Ductile Concrete Structures," *Proc. 8th Int'l Conf. on Creep, Shrinkage and Durability of Concrete and Concrete Structures*, Ise-Shima, Japan, Eds. Tanabe et al, Sept-Oct., 2008, pp. 761-768.

CHAPTER 9

Concluding Remarks

9.1 Research Overview and Findings

This dissertation focuses on the development and demonstration of an integrated multi-scale design framework for durable repair of concrete structures. This is accomplished through the establishment of links between the development, assessment, and implementation of an innovative material technology that fundamentally tackles major concrete deterioration problems. Within each of the design scales, the tailoring of ECC repair materials is highly focused on meeting specific structural performance requirements while adhering to additional system constraints (i.e. cost, processing, material availability, environmental exposure, existing cracks, etc.). A variety of micromechanics based tools, along with carefully designed experiments and finite element methods, are employed to understand and optimize ECC material development for specific repair applications. Furthermore, a comprehensive understanding of ECC material mechanical properties, durability, and its interaction with existing concrete under various environmental exposure and mechanical loading conditions is achieved in this

dissertation. In addition to laboratory development and experimental studies, the newly developed ductile repair technology is transferred to field implementation by optimizing workability and processing techniques, accommodating traditional large-scale mixing equipment, and demonstrating in a bridge repair project in Southern Michigan.

Research activities have been divided into individual chapters depending upon their placement within the overall integrated multi-scale design framework, namely material engineering (Chapters 2 and 3), repair system durability assessment (Chapters 4, 5, 6 and 7), and field application (Chapter 8). Significant findings and accomplishments made in individual research tasks are also summarized in the following.

9.1.1 Material Engineering for Durable Repair Materials

HES-ECC Material Development and Characterization

Material engineering for durable repair materials is possible through the application of micromechanical tools developed for ECC materials. This has been demonstrated through development of the ductile repair material High Early Strength ECC (HES-ECC) in Chapter 2. HES-ECC is designed for fast and durable repair of transportation infrastructure (e.g. bridges, roadways and highways), and other types of concrete structures that prefer a minimal interruption of operations and are often exposed to challenging environmental and mechanical loading conditions. Micromechanics can be used as a tool for designing HES-ECC composites that meet the two strain-hardening criteria as well as conditions for saturated multiple cracking, to achieve large tensile ductility above 3% and self-controlled crack widths below 100 μm at both early and late ages. These properties are crucial for repair durability, as they prevent cracking and

penetration of aggressive agents resulting from restrained volume change or stress concentration induced by pre-existing substrate cracks; cracking and aggressive agent penetration are typical deterioration causes in concrete repairs.

Through strategic combination of type III Portland cement, low water/cement ratio, polycarboxylate based superplasticizer and calcium nitrate based accelerator, and deliberate introduction of a small volume fraction (e.g. 5%) of PS beads, the newly developed HES-ECC material is capable of attaining compressive strength of 23.6 ± 1.4 MPa (3422 ± 203 psi) in 4 hours and 55.6 ± 2.2 MPa (8062 ± 315 psi) in 28 days, which generally exceeds federal and state transportation agency requirements. HES-ECC attains flexural strength of 9.8 ± 0.2 MPa (1422 ± 34 psi) in 4 hours and 15 ± 0.3 MPa (2187 ± 50 psi) in 28 days, which exceeds twice the flexural strength of concrete with similar compressive strength. Its tensile strength is 3.5 ± 0.1 MPa (501 ± 12 psi) at the age of 4 hours and 5.7 ± 0.2 MPa (823 ± 20 psi) at age of 28 days. The PS beads act as artificial flaws with controlled size and are included for maintaining tensile ductility of HES-ECC at all levels of maturity.

Detailed characterization of mechanical properties of HES-ECC further validated the material performance, and provided a database of the tensile, compressive, and flexural properties of the newly developed repair material for future engineering applications.

ECC Processing and Quality Control Optimized Material Properties and Robustness

ECC laboratory testing and application in construction projects will rely on the ability to consistently produce ECC materials with controlled quality. Chapter 3 focuses

on maximizing ECC material properties (e.g. tensile strain capacity, tensile strength) and minimizing material variation through a standardized processing technique. To achieve this, a simple and practical quality control method for ECC processing is developed in this chapter.

Through measurement of ECC mortar rheological parameters, fiber dispersion, and ECC tensile properties, correlations between these three quantities are established, which serve as a basis for identifying the optimal range of fresh properties for maximal hardened properties. During the rheology measurements, a strong correlation, with R = 0.95, is found between the Marsh cone flow time and plastic viscosity measured using a Viskomat-NT rotational viscometer, showing that the simple Marsh cone flow test should serve as a reliable indirect method for onsite or laboratory viscosity measurement. It is also found that incorporation of VMA can be an effective method to control plastic viscosity of ECC mortar without sacrificing ECC flowability after adding fibers.

The fluorescence imaging technique is a useful tool for quantifying the distribution of short discontinuous PVA fibers within a cementitious matrix. The fiber dispersion coefficient for seven mixes with the same mix design but increasing VMA content increases from 0.29 to 0.89. This quantifies the effectiveness of adding VMA as a new rheology control method for achieving more uniform fiber dispersion in hardened ECC, which has not been previously reported by other researchers.

Fiber uniformity, as measured by the fiber dispersion coefficient, has a strong effect on ECC tensile strain capacity. A lower fiber dispersion coefficient not only reduces ECC's tensile strain capacity and ultimate tensile strength, but also increases the variation in both properties. A very low value for the fiber dispersion coefficient can

switch ECC from a strain-hardening material to a tension-softening material. ECC mortar plastic viscosity is established experimentally as a fundamental rheological parameter that affects dispersion of PVA fibers in ECC mixes, and consequently affects ECC tensile strain capacity. An ECC mortar with low plastic viscosity and Marsh cone flow time tends to have poorly distributed fibers. Increasing plastic viscosity of ECC mortar improves fiber dispersion, and the improvement reaches a plateau once the Marsh cone flow time reaches 24 s. Further increasing viscosity can potentially lead to a reduction in ECC first cracking strength and ultimate tensile strength due to more larger-size entrapped air pores. Therefore, an optimal range of plastic viscosity (and corresponding optimal Marsh cone flow time) is revealed, which can be used to guide ECC rheology control during processing before fibers are added.

The present study results in a practical methodology to control the quality of ECC during laboratory or onsite large-scale processing for maximized material tensile properties and robustness, by simple use of a portable Marsh cone and adjustment of VMA content to result in a flow time between 24 s and 33 s. The effectiveness of this method was further confirmed using a special version of WHITE-ECC.

In summary of Chapter 2 and 3, for ECC to achieve robust tensile strain hardening behavior with designed tensile ductility, micromechanics-based material design should be combined with controlled material processing – neither of the two should be ignored. This is because material processing strongly affects the composite microstructure, which in turn determines whether the strain-hardening criteria are satisfied in the produced material as originally designed.

9.1.2 Durability Assessment of ECC/Concrete Repair System

Concrete repair failure results from a combination of physical, chemical and mechanical processes. Generally the repair deterioration process starts with repair cracking and repair/old interfacial delamination due to restrained volume change, or from reflective cracking due to stress concentration initiated in pre-existing cracks in substrate concrete. Cracking is an insidious cause of many repair durability problems, because it dramatically alters the transport properties of the repair material, facilitates the ingress of chloride into the repaired system, and eventually causes premature deterioration and repair failure such as corrosion and disintegration. At the repair system durability assessment level (middle triangle in Figure 1.10), the link between ECC repair material properties and repaired system durability is explored, in terms of the three major repair deterioration mechanisms: cracking and interfacial delamination due to restrained volume change (Chapter 4), reflective cracking (Chapter 5), and chloride penetration (Chapter 6).

Influence of Material Ductility on Restrained Volume Change Induced Cracking and Interfacial Delamination

Chapter 4 addresses one of the major durability concerns in concrete repairs, i.e. repair cracking and repair/old interfacial delamination due to restrained volume change and lack of dimensional compatibility. Through experimental, numerical and analytical studies of a simulated repair system under restrained shrinkage conditions, this chapter establishes conclusively that simultaneous suppression of repair cracking and interfacial delamination can be achieved using ductile ECC repair materials.

Specifically, the free drying shrinkage properties of HES-ECC (large compared

with normal concrete but below 0.3%) is found to be one order of magnitude lower than its tensile strain capacity of 3-6%. This leads to a highly negative cracking potential value, implying that when the drying shrinkage of HES-ECC is restrained, the material's ductility can accommodate shrinkage deformation by forming multiple microcracks during its strain-hardening stage without localized cracking failure. This contention is proven later by the results of the restrained shrinkage ring test and the restrained shrinkage test on a simulated repair system.

It is found that repair material ductility has a strong influence on the performance of the repaired system under restrained volume change. For a brittle repair material such as concrete or HES-Concrete, several localized surface cracks form with large width up to 520 μm, accompanied by a small amount of interfacial delamination up to 90 μm. A tension-softening repair material such as SFRC or HES-SFRC, which includes short steel fibers, is not able to suppress localized repair cracking with large crack width, although the presence of steel fibers does help to reduce the crack width to some extent. Meanwhile, the bridged cracks in an FRC greatly promote the tendency of interfacial delamination, which is the largest among the three categories of materials. This is because HES-SFRC has a positive cracking potential value with no inelastic strain capacity, so that the restrained shrinkage induced tensile and shear stresses at the interface have no avenue of release through material inelastic straining as does HES-ECC, or crack free-opening as does HES-Concrete. In contrast, a ductile repair material such as ECC or HES-ECC exhibits more than 100 fine microcracks with width less than 50 μm formed in the repair layer, accompanied by interface delamination less than 80 μm at the ends. The experimental results correspond well with the numerical simulation and a

simple analytical model developed in this study, concluding that the ductility of a repair material is the most essential factor contributing to the resistance to repair cracking and delamination.

This research departs from the traditional emphasis on isolated material properties such as high compressive strength and low shrinkage, and intends to shift the concrete repair industry's focus onto the age-dependent interaction between the new repair and old concrete. To ensure dimensional compatibility between the repair and existing concrete, a repair material with large inelastic tensile strain capacity (ductility) is necessary. When the material ductility requirement is satisfied, cracking control reinforcements and repair material free drying shrinkage limits will become less important, and surface preparation methods to enhance the interface bond will be more meaningful toward achieving durability of repaired concrete structures.

Although investigated in this study in the restrained shrinkage scenario, this concept of translating the ductility of the repair material to the durability of the repair system can be generalized to other restrained volume change (e.g. temperature effects) situations.

Influence of Material Ductility on Reflective Cracking in Overlay Repairs

Chapter 5 addresses the reflective cracking issues that are prevalent in concrete repairs – especially pavement overlay repairs. Reflective cracking is another major cracking mechanism that greatly affects concrete repair service life. It is caused by the brittle response of overlay material under high stress concentration induced by pre-existing joints or cracks in the substrate concrete. This chapter concludes that reflective

cracking can be fundamentally prevented through the high tensile ductility and strain-hardening behavior of ECC materials.

This was demonstrated in this study of an HES-ECC overlay system with an existing vertical crack in the substrate concrete and a small amount of interfacial delamination. Under monotonic and fatigue four-point bending, the HES-ECC overlay exhibited a "kinking and trapping" mechanism, and multiple microcracking behavior with controlled crack width below 50 μm (2×10^{-3} in.). Through this process a large amount of energy was dissipated, thus preventing the brittle reflective cracking failure mode that was observed in the control HES-Concrete overlay system.

Due to the ductile tensile behavior and unique "kinking and trapping" mechanism of the HES-ECC overlay, it exhibited 100% higher load carrying capacity and several orders of magnitude longer fatigue life compared to an HES-Concrete overlay with similar compressive strength and the same age. This suggests that significant improvements are possible in overlay design when HES-ECC is used: assuming the same loading conditions, (a) if designed with the same overlay thickness, the HES-ECC overlay is expected to have a significantly longer service life than traditional concrete overlays; (b) if designed with the same service life, the HES-ECC overlay thickness can be greatly reduced compared to traditional concrete overlays, leading to a significant amount of saving of materials, construction equipment, and construction time; or (c) a compromise of either parameter, i.e. reduced overlay thickness as well as prolonged overlay service life, can be achieved simultaneously.

It should be noted that the high resistance to reflective cracking of the HES-ECC overlay through multiple microcracking and the "kinking and trapping" mechanism is

also observed at the early age of 6 hours. The load carrying capacity of the HES-ECC overlay at the age of 6 hours and the control HES-Concrete overlay at the age of 28 days is almost the same. Furthermore, at the same stress level, the fatigue life of the HES-ECC overlay at the age of 6 hours is approximately one order of magnitude larger than that of the control HES-Concrete overlay at the same age. These results highlight the significant advantages of the newly developed HES-ECC material in fast and durable repair applications, with shortened operations shutdown time as well as greatly prolonged service life and increased load carrying capacity. These potentials in HES-ECC have not been demonstrated in other versions of ECC materials, or traditional concrete or FRC materials.

This methodology of suppressing reflective cracking can be generalized as translating the ductility of the repair material to the durability of the repair system, when subjected to stress concentration from existing cracks.

Transport Properties of ECC under Chloride Exposure

Chapter 6 addresses the chloride penetration stage in a typical repair deterioration process, before and after cracking occurs at different levels of strain. Chloride diffusion driven by a chloride concentration gradient, which is the predominant mechanism of chloride transport for most of the concrete structures exposed to deicing salts, and airborne or waterborne chloride ions, is the focus of this chapter.

Significant improvements in the resistance to chloride penetration can be achieved through the built-in microcracking mechanism of ECC materials. When subjected to increasing deformation levels, ECC exhibited multiple microcracking behavior with

increased crack numbers but self-controlled crack width under 50 μm (0.002 in.). This phenomenon is fundamentally different from traditional concrete repair materials, in which localized cracks form and the crack width enlarges with increasing strain level. Reinforcements can limit the width of such localized cracks to some degree, but will not alter the dependency of crack width on strain level and structural dimensions. This is partially illustrated in this study through testing on reinforced mortar specimens, which represent a large category of repair materials. After ECC beams and reinforced mortar beams are preloaded to various deformation levels, and subsequently exposed to 3% NaCl ponding for 90 days, the effective diffusion coefficient of ECC is measured to be significantly lower than that of reinforced mortar. Even at a twice-higher preloaded deformation level, the effective diffusion coefficient of the investigated ECC beam is around a quarter of that of the investigated reinforced mortar beam.

The significantly lower effective diffusion coefficient of ECC compared with reinforced mortar is attributed to the difference in cracking pattern. The effective diffusion coefficient of ECC is found to be linearly proportional to the number of cracks, whereas the effective diffusion coefficient of reinforced mortar is proportional to the square of the crack width. Therefore, crack width in mortar has a more pronounced effect on chloride transport than did the number of cracks in ECC, leading to a greatly higher effective diffusion coefficient at the same deformation level.

Additionally, through the formation of microcracks less than 50 μm (0.002 in.), a significant amount of self-healing was observed within the microcracked ECC when subjected to NaCl solution. This self-healing phenomenon aides in further reducing the effective diffusion coefficient of microcracked ECC.

In the uncracked beam specimens, the effective chloride diffusion coefficient of ECC is also lower than that of reinforced mortar for 30 and 90 days. This is explained by the denser microstructure of ECC due to a higher amount of cementitious materials, lower water/cementitious materials ratio, and high volume fly ash content. The immersion test results further prove this by comparing the chloride penetration depth in uncracked ECC and reinforced mortar.

The results show that ECC is effective at slowing down the diffusion of chloride ions under combined mechanical and environmental loading by virtue of its ability to achieve a self-controlled tight crack width, even under large applied strain levels. This study verifies the concept of improving repaired system durability with the inherent crack self-controlling mechanism of ECC repair materials.

Effect of Cracking and Healing on the Durability of ECC under Combined Aggressive Chloride Environment and Mechanical Loading

As the previous chapters (4, 5, and 6) concluded that ECC's large tensile ductility and self-controlled crack width below 100 μm are essential for achieving durable repair performance, Chapter 7 investigates the durability of ECC material itself in terms of maintaining its high ductility and tight crack width characteristics under combined mechanical loading conditions and aggressive chloride environmental conditions.

This study reveals that ECC maintained its unique tensile ductility and multiple microcracking behavior under combined mechanical loading conditions (0.5%, 1.0%, 1.5% tensile straining and reloading to failure) and aggressive chloride exposure (23-day, 60-day, and 90-day immersion in 3% NaCl solution). This indicates that even under

severe marine environment conditions, ECC remains durable and can provide reliable tensile ductility to prevent common cracking failure due to restrained volume change or stress concentration. Additionally, it maintains self-controlled microcrack width no larger than 100 μm during the material strain-hardening stage, and can thereby offer reliable resistance to chloride penetration even in severe marine environment conditions.

Micromechanical scale experimental studies are carried out to understand the observed composites behavior. After exposure to 3% NaCl solution for 30, 60 and 90 days, changes in ECC matrix fracture toughness, interfacial chemical bond, and interfacial frictional bond are experimentally determined and compared with those of ECC without exposure to NaCl. These changes are due to the presence of chloride ions, which tend to increase the leaching of calcium hydroxide and porosity. The reduction in fiber/matrix interfacial bonds explains the increase in average crack width of ECC from 45 μm (before chloride exposure) to 100 μm (after chloride exposure for 30, 60 and 90 days); the reduction in matrix fracture toughness explains the reduction in ultimate tensile strength after chloride exposure for 30, 60 and 90 days. Interestingly, the simultaneous decreases in fracture toughness and interfacial bonds result in an unchanged (or slightly increased) PSH pseudo strain-hardening index (J_b'/J_{tip}), leading to a non-deteriorated tensile strain capacity of ECC after 30-day, 60-day, and 90-day chloride exposures.

The innately tight crack width in ECC is favorable for the self-healing process to take place. This is demonstrated in Chapter 6 in terms of recovery of chloride transport properties, and then in Chapter 7 in terms of recovery of tensile behavior. Specimens preloaded to 1.5% strain nearly completely recover their stiffness and tensile strain

capacity when reloaded in direct tensile tests, even after periods of 30, 60, and 90 days exposure to NaCl solution.

9.1.3 Field Application of ECC Repair Materials

Chapter 8 shifts the focus from "repair system durability assessment" to the "structural application" portion of the integrated engineering methodology (upper triangle in Figure 1.10). Efforts are made to transfer innovative ECC repair technology from the laboratory to field implementation through a bridge patch repair demonstration project.

Before the newly-developed HES-ECC material can be considered a viable building material for use in repair or structural designs, it must be capable of processing at a large scale using commercial batching equipment common within the repair construction industry. In this chapter, large-scale processing and construction of an HES-ECC repair using commercial facilities are realized through optimization of the HES-ECC ingredients and mixing procedure, trial batches, and quality control methods.

Specifically, workability of HES-ECC is evaluated with scaled-up batching sizes. Gravity mixers are used to process HES-ECC at batch sizes of 1, 3 and 6 cubic feet (0.03, 0.08, 0.17 cubic meters). Prior to the larger scale batching, preliminary tests in the laboratory are carried out to improve flowability and workability of the material. The 0.5 in. (12.7 mm) long PVA fiber used previously in HES-ECC is changed to 0.33 in. (8.4 mm) long PVA fiber to promote easy mixing and better fiber distribution in the gravity mixer, and to improve flowability of the material. Additionally, the effect of the hydration stabilizer on the flowability, initial setting time, and hardened mechanical

properties of HES-ECC is evaluated. Finally, the batching sequence of this material is also optimized to facilitate mixing based on larger scale gravity mixers.

Based on the results from 1, 3 and 6 cubic feet (0.03, 0.08, and 0.17 cubic meter) trial batches, it is concluded that larger scale mixing of HES-ECC material approaching that of field conditions can be accomplished without difficulty. Using the optimized batching sequence, the overall mixing of HES-ECC material proceeds smoothly and results in a fresh material that is homogeneous, flows well, and is rheologically stable. Testing of hardened mechanical properties of HES-ECC processed in 1, 3 and 6 cubic feet (0.03, 0.08, and 0.17 cubic meter) batching, shows that the early age and late age compressive strength and tensile strain capacity are similar to those of mixes made in a laboratory size Hobart mixer, and continue to meet all of the performance targets set forth when developing HES-ECC at the laboratory scale.

A HES-ECC patch repair was constructed on the Ellsworth Road Bridge over US-23 (S07 of 81074) on November 28, 2006. A 7 cubic foot (0.20 cubic meter) HES-ECC batch was mixed by MDOT and UM research personnel using a 12 cubic foot (0.34 cubic meter) capacity concrete gas mixer provided by MDOT. The mixing time was approximately 30 minutes. The mixed HES-ECC exhibited desirable creamy viscosity, good fiber distribution, and self-compacting properties. The repair construction was completed at around 1pm on Tuesday, November 28, 2006. Traffic reopened at 9am on Wednesday, November 29, 2006.

The long-term durability of the HES-ECC patch repair under field conditions was monitored until September 18, 2009. Under heavy traffic loading, shrinkage, temperature effects, three winters' exposure to freezing and thawing as well as de-icing salts, and

other possible loading conditions in field, the HES-ECC patch repair exhibited multiple microcracking behavior with crack width below 100 μm, and no sign of disintegration and fracture failure. Through this work, the linkages between material engineering, repair system durability assessment, and structural application are further forged.

9.2 Impact of Research

Lack of durability in concrete infrastructure has become a looming threat that could jeopardize the world's prosperity and our quality of life. According to the American Society of Civil Engineers (ASCE) 2009 Report Card[1] for US Infrastructure, an average grade of D (poor) was assigned over 12 infrastructure categories. ASCE estimated that USD 2.2 trillion is needed over the next five years for repair and retrofit. Correspondingly, repair and retrofit cost has been estimated to be USD 2 trillion for Asia's infrastructure. In Europe, Japan, Korea, and Thailand, the annual cost for repair has exceeded that for new construction[2].

While countless materials and techniques are used in practice to meet the demand for rapid, inexpensive and durable concrete repairs, few of them target the inherent material shortfall of concrete as a brittle material that cracks and fractures in many applications, leading to further deterioration. It has been estimated that almost half of all concrete repairs fail prematurely[3]. The challenges posed by deteriorating concrete structures and widely-observed repair failures require an effective and practical approach that breaks down the concrete deterioration process, which typically begins with restrained volume change induced cracking or reflective cracking, followed by penetration of aggressive agents, and eventually results in concrete spalling,

disintegration, and loss of structural capacity. The current repair materials and technologies have had limited success in preventing these deterioration mechanisms.

The main contribution of this dissertation is to develop and implement a novel integrated multi-scale design framework for durable concrete repairs, which addresses the aforementioned limitations of current repair technologies. This framework begins with material microstructure tailoring at the micrometer scale, links to repaired system durability assessment through composite material properties at the centimeter scale, and ultimately relates construction processes and performance evaluation at the meter scale of the repaired infrastructure. To achieve the holistic durability of such engineered systems, durability concepts are interwoven across all material engineering, system durability assessment, and structural application scales.

As opposed to traditional concrete and fiber reinforced concrete (FRC) materials that are susceptible to cracking and fracture failure, a new class of innovative, ductile ECC repair materials can be designed using micromechanics and processing tools offered by material engineering technology to exhibit desired multifunctionality (i.e., possessing more than one of the engineering functionalities) that addresses each typical deterioration stage in concrete repairs. The main differences between the new and traditional concrete repair materials are that the former possesses more than 300% larger tensile strain capacity, inherent self-controlled crack width under 100 μm without relying on steel reinforcement, and great tailor-ability with additional functionalities (e.g. high early strength) based on established micromechanics tools. These properties, as revealed and validated in this dissertation, are essential for suppressing the three major concrete deterioration mechanisms, namely (a) cracking and interfacial delamination due to

restrained volume change, (b) reflective cracking due to stress concentration from existing cracks, and (c) chloride penetration that initiates embedded steel corrosion. Without these properties, traditional repair materials and technologies can only delay, but not fundamentally suppress, concrete deterioration.

The capability of consistently processing and producing robust ECC materials plays a crucial role in its ascendancy as a new construction material in various structural applications. To address this need, this dissertation develops a practical quality control approach for laboratory or onsite ECC processing in order to maximize material properties as designed, and minimize material variation. This approach is novel, in that it is based on the systematically-built relationship between ECC material fresh rheological properties, dispersion uniformity of short PVA fibers within the cementitious matrix, and ECC material hardened tensile properties. As opposed to qualitative approaches that have previously been used often in ECC processing, which involve visual and physical (by hand) inspection of mix homogeneity and fiber dispersion uniformity, this approach offers a quantitative and scientifically-based method that relates the marsh cone flow rate to fiber dispersion coefficient. Furthermore, this dissertation brings to attention that non-uniform fiber dispersion within ECC can result in undesirable variation in its tensile properties, and even switch ECC from a strain-hardening material to a tension-softening normal fiber reinforced concrete (FRC) material. This can lead to material properties that fall short of those originally designed for using the ECC micromechanical theory, which assumes uniform fiber dispersion.

This dissertation also provides a comprehensive understanding on the deterioration mechanisms of concrete repairs under various environmental and

mechanical loading conditions. Through identifying causes and effects of each deterioration stage, the critical repair material properties that influence each stage are determined. The influence of material properties on the interaction between the repair and the existing concrete as well as the durability of the repair system is addressed. Finally, the performance and practicality of this material technology is justified not only in laboratory studies, but also in field full-scale application.

This dissertation departs from the traditional emphasis on isolated material properties such as high compressive strength and low shrinkage, and intends to shift the repair industry's attention toward the age-dependent interaction between the new repair and old concrete. This concept of translating the ductility of the repair material to the durability of the repair system, at different deterioration stages (i.e. restrained shrinkage cracking, interfacial delamination, reflective cracking, chloride penetration, fatigue, loss of durability in aggressive chloride environment) can be widely applied to concrete structure repair applications for minimizing maintenance requirements and reducing repair costs. The potential impacts of the integrated multi-scale design framework on society's ability to preserve and extend service life of large volume of existing concrete infrastructure systems, which represent less harm to future generations in terms of economic, social and environmental impacts, are indeed tremendous.

9.3 Recommendations for Future Research

Different from new construction, successful concrete repairs require an accurate understanding of the underlying concrete deterioration mechanisms and causes and effects, which can be case-sensitive based on specific environmental, loading, and

boundary conditions. While the development of HES-ECC was successfully completed for fast and durable repair applications, which cover a broad range of transportation infrastructure and other types of structures that prefer minimal operations disruption, other repair scenarios are still open to consideration. For example, repair of damaged concrete members due to earthquake, fire, or impact loading may need additional repair material properties to meet specific requirements, such as resistance to high strain-rate loading, or non-deterioration in fiber and fiber/matrix interfacial properties under very high temperature. Additionally, for repair of non-critical structures, while compressive strength requirements are lower, ECC materials with mix designs incorporating large volumes of waste materials (e.g. fly ash, slag, rice husk ash) may be preferable to mixes with the lowest initial cost or highest material greenness. Finally, for regions where only local ingredients are available, strategic incorporation of these local ingredients into ECC materials, without sacrificing critical material properties that are desired for repair durability, will be meaningful.

This dissertation investigated three major deterioration mechanisms in concrete repairs: repair cracking and interfacial delamination due to restrained volume change, overlay reflective cracking, and chloride penetration. However, there are other deterioration mechanisms that need to be better understood in the future, such as alkali silica reaction, salt-scaling, concrete spalling and loss of load carrying capacity due to steel corrosion, and accelerated corrosion in concrete repairs. Furthermore, combined loading states consisting of mechanical and environmental loads, instead of single deterioration mechanisms, need to be more comprehensively considered in future studies of concrete repair durability and service life estimations.

Accelerated corrosion in concrete repairs due to electrochemical incompatibility between "old" and "new" portions of the repaired concrete structures is commonly present[4]. The effect of a repair on electrochemical activity in a repaired structure is a function of the change in voltage potentials, the nature of the repair materials, and the exterior and interior environments. If the steel in the repair area is partially embedded in existing, chloride-contaminated concrete, and partially in new repair material, strong corrosion cells can develop. The part of the steel bar in the existing concrete will become anodic and corrode at a rapid rate, driven by the other part acting as a cathode. In this case, repair phase deterioration and failure may develop in less than 1 year. Such an accelerated corrosion process can be influenced by the cracking pattern of repair materials. Chloride ions penetrate fastest through cracks, reach the embedded steel, and turn these parts of steel into anodes. The number of cracks, and the chloride penetration rate through cracks, will determine whether microcells or macrocells will form and the rate of corrosion. Therefore, the effects of ECC multiple microcracking behavior, in contrast with the localized cracks with larger crack width (higher chloride diffusion rate) in traditional concrete repairs, on modifications of the accelerated corrosion process will be of great research interest.

Broader impacts (i.e. economic, social, and environmental impacts) resulted from increased durability of concrete structures containing alternative ECC repair materials, compared with those containing traditional materials, need to be quantified through life-cycle modeling and analysis. The development and validation of service life models comprise large opportunities for future research. For example, the measured effective diffusion coefficient of ECC materials in this dissertation compared with traditional

reinforced mortar materials can be used for future service life prediction and life cycle cost analysis of ECC repairs or structures. While the methods can focus on a single deterioration mechanism resulting in the most common failure mode, concrete repairs can fail in a variety of ways at any age. A probabilistic-based model for use in predicting the service life of concrete repairs and repaired structures is needed. At this time, few of these values have been incorporated in service life models or established for new materials such as ECC.

The self-healing phenomenon under chloride exposure was revealed in this dissertation in terms of recovery of both chloride transport properties and material tensile properties. The self-healing mechanism under chloride exposure might be different from other exposure conditions (e.g. immersion in water, wet-dry, high alkali environment), and would be of research interest. The physical and chemical mechanisms behind the self-healing phenomena need to be understood at the micro-scale level. For example, the details of the ECC self-healing process and self-healing product need to be examined through ESEM (Environmental Scanning Electron Microscope) and X-ray diffraction technology. The mechanical properties of self-healing products and their influence on ECC micro-parameters (i.e. matrix fracture toughness, fiber/matrix chemical bond, frictional bond and slip-hardening coefficient) need to be quantified to guide ingredient re-selection and material microstructure tailoring to further ensure robust self-healing. At the macro-scale level, the repeatability of self-healing is still unknown. Also, the laboratory self-healing test was performed in the unloaded state. Given that structures in the field are likely to be in the loaded state, self-healing behavior in the loaded state will need to be evaluated and established. In addition, ECC self-healing under field

conditions has never been demonstrated and needs to be further confirmed both in the loaded and unloaded state.

More field demonstration projects and repair applications of ECC materials are needed in the future to evaluate their performances under various field environmental and mechanical loading conditions, repair dimension scales, and boundary conditions. Further exploration of the links between material engineering, system durability assessment, and structural application within the multi-scale design framework will be greatly meaningful.

References:

[1] Report Card for America's Infrastructure. 2009. http://www.infrastructurereportcard.org/

[2] Li, V. C., "Engineered Cementitious Composites", *Proceedings of ConMat'05*, Vancouver, Canada, August 22-24, 2005, CD-documents/1-05/SS-GF-01_FP.pdf.

[3] Vaysburd, A. M., Brown, C. D., Bissonnette, B, and Emmons, P. H., ""Realcrete" versus "Labcrete"", *Concrete International*, Vol. 26, No.2, 2004, pp. 90-94.

[4] Vaysburd, A. M., and Emmons, P. H., "How to Make Today's Repairs Durable for Tomorrow – Corrosion Protection in Concrete Repair," *Construction and Building Materials*, Vol. 14, No. 20, 2000, pp. 189-197.